J. Fluid Mech. (1995), *vol.* 292, *pp.* 271–304

Influence of incidence angle on sound generation by airfoils interacting with high-frequency gusts

By MATTHEW R. MYERS[1] AND E. J. KERSCHEN[2]

[1] Hydrodynamics and Acoustics Branch, US Food and Drug Administration, HFZ-132, Rockville, MD 20817, USA

[2] Aerospace and Mechanical Engineering Department, University of Arizona, Tucson, AZ 85721, USA

(Received 10 November 1993 and in revised form 20 January 1995)

A theoretical model is developed for the sound generated when a convected vortical or entropic gust encounters an airfoil at non-zero angle of attack. The theory is based on a linearization of the Euler equations about the steady subsonic flow past the airfoil. High-frequency gusts, whose wavelengths are short compared to the airfoil chord, but long compared to the displacement of the mean-flow stagnation point from the leading edge, are considered. The analysis utilizes singular-perturbation techniques and involves four asymptotic regions. Local regions, which scale on the gust wavelength, are present at the airfoil leading and trailing edges. Behind the airfoil a 'transition' region, which is similar to the transition zone between illuminated and shadow zones in optical problems, is present. In the outer region, far away from the airfoil edges and wake, the solution has a geometric-acoustics form. The primary sound generation is found to be concentrated in the local leading-edge region. The trailing edge plays a secondary role as a scatterer of the sound generated in the leading-edge region. Parametric calculations are presented which illustrate that moderate levels of airfoil steady loading can significantly affect the sound field produced by airfoil–gust interactions.

1. Introduction

The unsteady interaction of airfoils with convected disturbances is a phenomenon that occurs in a wide variety of technological applications. This interaction is responsible for much of the sound generated by aeronautical propulsion systems and for unsteady blade loading which may lead to fatigue failures in these systems. In many applications, the airfoils have substantial levels of steady aerodynamic loading. However, the airfoil steady loading, and the attendant distortions of the mean flow, are often ignored in noise-prediction analyses. The present paper examines the influence of mean incidence angle on sound generated by the interaction of convected disturbances with a flat-plate airfoil. The mean flow is assumed to be compressible but subsonic, and attention is concentrated on the high-frequency situation where the gust wavelength is short compared to the airfoil chord.

Most analyses of airfoil–gust interactions have utilized the classical linearized approach, in which the total flow is represented as the sum of a uniform flow, an $O(\alpha)$ (relative to the uniform field) steady disturbance, and an $O(\epsilon)$ unsteady disturbance. If one assumes that α and ϵ are small and comparable, in analysing the unsteady flow it is natural to neglect the $O(\alpha)$ corrections to the steady flow. The unsteady calculation

then corresponds to a small perturbation of a uniform flow, which simplifies the analysis considerably. However, in many cases $\alpha \gg \epsilon$, and it then becomes desirable to include the effects of the mean flow distortion on the unsteady motion.

The significance of steady-loading effects on sound generated by airfoil–gust interactions was first recognized by Ffowcs Williams & Hawkings. They developed an elegant extension of Lighthill's acoustic analogy (Ffowcs Williams & Hawkings 1969*a*) which accounted for the presence of surfaces in arbitrary motion. In a subsequent paper (Ffowcs Williams & Hawkings 1969*b*), they utilized this theory to show that airfoil steady loading produces a quadrupole source related to the Reynolds stresses arising from interactions of the convected gust with gradients of the mean flow. Subsequently, Ffowcs Williams & Hall (1970) examined the scattering of a 'free' quadrupole field by an extended surface with a sharp edge. They found that, at sufficiently low flow speeds, this scattered field due to the sharp edge dominates over the contribution from the surface dipole terms. The theory developed in the present paper examines the influence of airfoil steady loading from a different point of view, but in the proper limit will be seen to have much in common with the quadrupole theories of Ffowcs Williams.

The acoustic analogy is an exact statement of the laws governing the fluid motion, cast in the form of a constant-coefficient linear wave operator with a quadrupole source term representing nonlinear and other effects. However, sound predictions utilizing the acoustic analogy require the source term to be modelled, since its exact form can be found only by solving the original nonlinear fluid-dynamic equations. Most models of the quadrupole source terms for airfoil–gust interactions have been quite simplistic. For example, Ffowcs Williams & Hawkings (1969*b*) simply replaced the distributed sources by a single concentrated source, while Goldstein, Rosenbaum & Albers (1974) modelled the airfoils as point vortices. Such approximations have value at low frequencies where the source region is compact, i.e. small compared to the acoustic wavelength. The present paper addresses the high-frequency case where the source region is highly non-compact and modelling of the quadrupole source terms is more difficult.

Our theory utilizes an alternative formulation for analysing the interaction of bodies with convected disturbances. This formulation is an extension of classical rapid-distortion theory (Batchelor & Proudman 1954), initiated by Hunt (1973) for incompressible flows and modified and extended to compressible flows by Goldstein (1978). Rapid-distortion theory considers inviscid linear unsteady disturbances to an irrotational base flow. Thus it accounts for the distortion of vorticity by mean-flow gradients, but neglects viscous effects and the nonlinear interactions between the disturbance quantities. In contrast to the acoustic analogy, in the present approach the source terms which arise in the governing equations are known precisely, and hence no heuristic modelling is required.

Rapid-distortion theory has previously been utilized to study the interaction of airfoils with convected disturbances in the incompressible flow limit. Goldstein & Atassi (1976) and Atassi (1984) considered two-dimensional flow, and developed the first-order correction to the unsteady flow in the limit of small reduced frequency. Less progress has been made for the case of compressible mean flows. Goldstein's (1978) formulation reduces the problem to the solution of a single linear convected-wave equation with specified source terms and boundary conditions, but for a compressible mean flow the equation has variable coefficients. These variable coefficients, as well as functions appearing in the source term and boundary conditions, must in general be determined numerically. A numerical solution of the rapid-distortion equations for the

sound field produced by compressible airfoil–gust interactions was presented by Scott & Atassi (1990) and Atassi, Subramaniam & Scott (1990).

For a compressible mean flow which is a small perturbation to a uniform flow, Kerschen & Myers (1987) derived approximate closed-form expressions for all the functions which appear in Goldstein's formulation. The present paper utilizes the result of Kerschen & Myers (1987) to develop approximate closed-form expressions for the sound field produced by convected disturbances interacting with a flat-plate airfoil in compressible flow. A complete theory that includes the first-order effects of airfoil steady loading is developed. The theory is a systematic asymptotic expansion which contains no heuristic modelling. The analysis uses a combination of complex-variable and singular-perturbation techniques. We consider short-wavelength gusts and small incidence angles. The theory is linear in the gust amplitude ϵ, which is assumed to be very small compared to the $O(\alpha)$ mean-flow disturbance.

Our results indicate that aerodynamic loading values typically found in turbomachinery have significant effects on the radiated sound. Comparisons with the acoustic-analogy approach are also made. Certain characteristics predicted by the earlier acoustic-analogy models are recovered, confirming the physical mechanisms proposed by Ffowcs Williams. New features of the physics are also found, illustrating the importance of propagation effects which are often ignored in models based on the acoustic analogy.

2. General formulation

The analysis considers inviscid linear disturbances of a two-dimensional irrotational compressible mean flow, utilizing the formulation developed by Goldstein. Small-amplitude vortical and entropic disturbances are assumed to be present in the uniform flow far upstream of the airfoil. These disturbances convect downstream and interact with the airfoil, generating sound in the process.

Goldstein (1978) showed that the analysis of the unsteady motion could be reduced to the solution of a single inhomogeneous convected-wave equation. His formulation utilizes a decomposition of the unsteady velocity disturbance in the form

$$\boldsymbol{u}' = \nabla G' + \boldsymbol{v}', \tag{2.1a}$$

where it should be noted that $\boldsymbol{v}'$ is not solenoidal. Rather, $\boldsymbol{v}'$ satisfies a modified form of the linearized momentum equation which can be integrated exactly using the method of characteristics. Thus $\boldsymbol{v}'$ is a known function which contains the upstream vorticity and the additional vorticity generated by interaction of the upstream disturbances with the mean-flow gradients. The irrotational field satisfies (Goldstein 1978)

$$\frac{\mathrm{D}_0}{\mathrm{D}t}\left(\frac{1}{a_0^2}\frac{\mathrm{D}_0 G'}{\mathrm{D}t}\right) - \frac{1}{\rho_0}\nabla\cdot(\rho_0 \nabla G') = \frac{1}{\rho_0}\nabla\cdot(\rho_0 \boldsymbol{v}'), \tag{2.1b}$$

and the pressure is prescribed by

$$p' = -\rho_0 \mathrm{D}_0 G'/\mathrm{D}t. \tag{2.1c}$$

The substantial derivative $\mathrm{D}_0/\mathrm{D}t$ is taken with respect to the local mean flow. The quantities ρ_0 and a_0 are the local values of density and speed of sound for the mean flow. The boundary condition on G' at any rigid surface is

$$\partial G'/\partial n = -\boldsymbol{v}'\cdot\boldsymbol{n}, \tag{2.1d}$$

where $\boldsymbol{n}$ is the unit normal vector. The radiation condition applies at infinity.

For incompressible flow, (2.1*b*) reduces to a Poisson equation. For the compressible case, the mean-flow quantities which appear in (2.1*b*) must in general be determined numerically, precluding the possibility of an analytical solution. Therefore, we will consider a simplified form of (2.1*b*) which assumes that the mean flow is a small ($O(\alpha)$) perturbation of a uniform flow (Kerschen & Myers 1987).

Since vorticity and entropy disturbances convect with the (non-uniform) mean flow, it proves convenient to introduce the mean-flow velocity potential and streamfunction, and the spanwise position x_3, as orthogonal curvilinear coordinates. We set

$$\phi = \phi_p/U_\infty b, \quad \psi = \beta_\infty \psi_p/U_\infty b, \quad x_3 = x_{3p}/b. \tag{2.2a}$$

Here ϕ_p and ψ_p are the physical velocity potential and streamfunction, x_{3p} the dimensional spanwise coordinate, U_∞ the speed of the uniform mean flow far from the airfoil, and b the airfoil semi-chord. The introduction of the factor $\beta_\infty = (1-M_\infty^2)^{1/2}$ ($M_\infty = U_\infty/a_\infty$) in the definition of ψ corresponds to a Prandtl–Glauert transformation (Ashley & Landahl 1985). The appropriate coordinate metrics are

$$m_\phi = \frac{bU_\infty}{U_0}, \quad m_\psi = \frac{b\rho_\infty U_\infty}{\beta_\infty \rho_0 U_0}, \quad m_3 = b, \tag{2.2b}$$

where U_0 is the local speed of the mean flow.

The unsteady disturbances satisfy linear equations whose coefficients are constant in regions where the mean flow is uniform. Hence, we can represent arbitrary upstream disturbances as a superposition of harmonic components, and develop the solution for a single harmonic component. The upstream velocity and entropy disturbances are then given by

$$\begin{bmatrix} \boldsymbol{v}' \\ s' \end{bmatrix} = \begin{bmatrix} \epsilon U_\infty (A_t, A_n, A_3) \\ 2\epsilon c_p B \end{bmatrix} e^{ik(\phi + k_n \psi + k_3 x_3 - t)}, \tag{2.3a,b}$$

where

$$k = \omega b/U_\infty \tag{2.3c}$$

is the reduced frequency of unsteady aerodynamic theory, time is normalized by b/U_∞, and c_p is the specific heat at constant pressure. The dimensionless parameter ϵ is assumed to be small. In anticipation of the high-frequency analysis, we have expressed the ψ and x_3 wavenumber components in terms of k, which subsequently will be assumed large. Far upstream the vortical velocity must be solenoidal, hence

$$A_t + A_n k_n \beta_\infty + A_3 k_3 = 0. \tag{2.3d}$$

In order to obtain closed-form analytical approximations for the coefficients and source term in (2.1*b*), we assume that the mean flow is a small perturbation, say $O(\alpha)$ to a uniform flow, with $\epsilon \ll \alpha \ll 1$. The mean-flow disturbance can then be described by a complex potential $\alpha F(\zeta)$, where $\zeta = \phi + i\psi$, and the function F can be obtained from incompressible theory (Ashley & Landahl 1985). Specifically, if the complex disturbance potential for the corresponding incompressible flow is $\alpha F_i(x_p + iy_p)$, where (x_p, y_p) are physical coordinates non-dimensionalized by b and F_i is normalized by bU_∞, the appropriate compressible complex potential in the present coordinates is

$$\alpha F = \frac{\alpha}{\beta_\infty} F_i(\phi + i\psi) + O(\alpha^2).$$

Upon setting the derivative $dF(\zeta)/d\zeta$ equal to $q - i\mu$, we identify q as the normalized perturbation in flow speed:

$$U_0/U_\infty = 1 + \alpha q(\phi, \psi) + O(\alpha^2),$$

and $\alpha\beta_\infty \mu$ as the perturbation in flow angle in the physical plane.

By introducing the transformation

$$\frac{G'}{\epsilon U_\infty b} = h(\phi,\psi)\,\mathrm{e}^{\mathrm{i}k(k_3 x_3 - t)}\,\mathrm{e}^{-\mathrm{i}kM_\infty^2\phi/\beta_\infty^2}\,\mathrm{e}^{\alpha M_\infty^2 q} \tag{2.4a}$$

and neglecting $O(\alpha^2)$ terms, Kerschen & Myers (1987) simplified Goldstein's wave equation (2.1*b*) to

$$\mathrm{L}_0(h)+\alpha\mathrm{L}_1(h) = \alpha k S(\phi,\psi)\,\mathrm{e}^{\mathrm{i}k\Omega}. \tag{2.4b}$$

The operator L_0 is the standard Helmholtz operator

$$\mathrm{L}_0(h) = \frac{\partial^2 h}{\partial\phi^2}+\frac{\partial^2 h}{\partial\psi^2}+k^2w^2h, \tag{2.4c}$$

where

$$w^2 = (\delta M_\infty)^2-(k_3/\beta_\infty)^2$$

and $\delta = 1/\beta_\infty^2$. The operator L_1 contains variable coefficients, and accounts for effects of the mean-flow gradients on the acoustic propagation. This operator takes the form

$$\mathrm{L}_1(h) = \frac{(\gamma+1)M_\infty^4}{\beta_\infty^2}\left\{q\left[\frac{\partial^2 h}{\partial\psi^2}+2\mathrm{i}k\delta\frac{\partial h}{\partial\phi}+k^2(w^2+\delta^2)h\right]-\frac{\partial q}{\partial\phi}\left[\frac{\partial h}{\partial\phi}-\mathrm{i}k\delta h\right]\right\}-2k^2w^2\beta_\infty^2 qh. \tag{2.4d}$$

Note that the coefficients in L_1 depend on ϕ and ψ only through the normalized perturbation in flow speed $q(\phi,\psi)$. The amplitude $S(\phi,\psi)$ of the source term in (2.4*b*) is given by

$$S(\phi,\psi) = \frac{2}{\beta_\infty^2}\left\{\mathrm{i}(A_t^*-k_n A_n\beta_\infty^3)q+\mathrm{i}(k_n A_t^*\beta_\infty^2+A_n\beta_\infty)\mu\right.$$
$$\left.+\frac{1}{k}\left[A_t^* M_\infty^2\frac{\partial q}{\partial\phi}+A_n M_\infty^2\beta_\infty\frac{\partial q}{\partial\psi}\right]\right\}, \tag{2.5a}$$

where $A_t^* = A_t - B$. The phase of the source term is

$$\Omega = \delta\phi+k_n\psi+g(\phi,\psi), \tag{2.5b}$$

where

$$g(\phi,\psi) = \int_{-\infty}^{\phi}\left[\frac{U_\infty^2}{U_0^2(\eta,\psi)}-1\right]\mathrm{d}\eta. \tag{2.5c}$$

The integral $g(\phi,\psi)$ is Lighthill's Drift function, which represents the cumulative distortion of vortex filaments by the non-uniform mean flow. For a mean flow which is a small perturbation of a uniform flow, g can be approximated by (Kerschen & Balsa 1981)

$$g(\phi,\psi) = -\alpha 2\,\mathrm{Re}\,[F(\zeta)], \tag{2.5d}$$

where the arbitrary constant in the complex potential $F(z)$ is chosen such that the Drift function vanishes at upstream infinity.

The boundary condition (2.1*d*) transforms to

$$\frac{\partial h}{\partial\psi}+\alpha M_\infty^2\frac{\partial q}{\partial\psi}h = -\left[\frac{A_n}{\beta_\infty}(1-\alpha M_\infty^2 q)-\alpha 2A_t^*\mu\right]\mathrm{e}^{\mathrm{i}k\Omega}, \tag{2.6}$$

applied on the body surface. The terms in (2.6) containing M_∞^2 have arisen from the factor $\mathrm{e}^{\alpha M_\infty^2 q}$ in the transformation (2.4*a*) from G' to h. This factor, which simplifies the

differential operator L_1, transfers to the boundary condition some of the influence of mean-flow gradients in the wave operator of (2.1*b*).

To prescribe the pressure in terms of the modified potential h, we utilize (2.4*a*) in (2.1*c*) and find

$$p' = -\epsilon\rho_\infty U_\infty^2 \left\{\left[\frac{\partial h}{\partial \phi} - ik\delta h\right] e^{ik(k_3 x_3 - t - \delta M_\infty^2 \phi)} + O(\alpha)\right\}. \tag{2.7}$$

It will be useful to work in terms of the modified pressure p, defined by

$$p = \frac{-p' e^{ik(-k_3 x_3 + t)}}{\epsilon\rho_\infty U_\infty^2} = \left[\frac{\partial h}{\partial \phi} - ik\delta h\right] e^{-ik\delta M_\infty^2 \phi}. \tag{2.8}$$

The analysis thus far applies to a general small-perturbation mean flow. In the remainder of this paper, we concentrate on the sound field generated by the interaction of convected disturbances with a flat-plate airfoil at non-zero incidence angle, α.

3. Analysis for a flat plate

We consider a flat plate of length $2b$ at mean incidence angle α to a uniform stream, interacting with a time-harmonic convected disturbance whose wavelength is short compared to the airfoil chord. The problem is illustrated in figure 1. The $O(\alpha)$ perturbations to the mean flow appearing in (2.4)–(2.6) are then given by the complex potential

$$F(\zeta) = \frac{i}{\beta_\infty}(\log[\zeta - 1 + [\zeta(\zeta-2)]^{1/2}] + \zeta - [\zeta(\zeta-2)]^{1/2} + C) \tag{3.1a}$$

and complex velocity

$$F'(\zeta) = q - i\mu = \frac{i}{\beta_\infty}[1 - ((\zeta-2)/\zeta)^{1/2}]. \tag{3.1b}$$

The function F appears in several places in our analysis; the arbitrary constant C will be specified for each application. The airfoil surface in the (ϕ, ψ)-plane is given by $0 < \phi < 2 \pm \alpha\pi/\beta_\infty$, $\psi = 0^\pm$. The location of the trailing edge is different for the upper and lower surfaces, owing to the net circulation.

We develop an asymptotic solution to (2.4*b*) for small α and large k. The asymptotic expansion has a singular-perturbation nature, and involves four different regions whose sizes are controlled by the reduced frequency. The various asymptotic regions are illustrated in figure 2. The appropriate lengthscale in the local regions near the airfoil leading and trailing edges is the disturbance wavelength. Since we assume that M_∞ is $O(1)$, the wavelengths of the convected and acoustic disturbances have the same order of magnitude. In the outer region away from the airfoil leading and trailing edges, the mean flow varies slowly compared to the disturbance wavelength and the solution has a geometric-acoustics form. In addition, there is a 'transition region' of $O(k^{-1/2})$ angular extent downstream of the airfoil. Here the multiple-scale dependence of the outer region applies in the streamwise direction, but a rescaled transverse coordinate is required to describe the transition between the ray fields which have propagated along the upper and lower surfaces of the airfoil.

A further assumption $\alpha^2 k \ll 1$ is utilized in the analysis. For a flat-plate airfoil at small incidence angle, the shift in the mean-flow stagnation point from the leading edge is $O(\alpha^2 b)$. Thus, this assumption implies that the shift of the mean-flow stagnation point is small compared to the disturbance wavelength. In practical terms, wavelengths

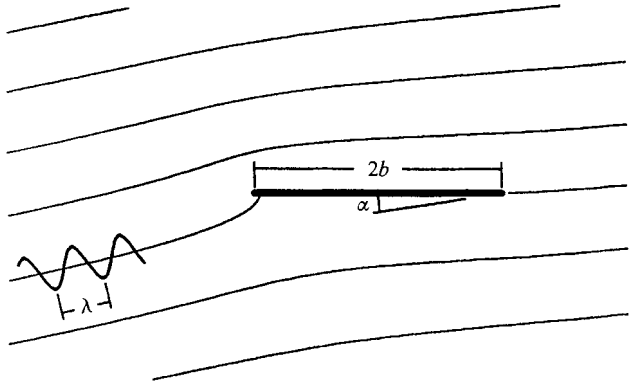

FIGURE 1. Flat-plate airfoil at incidence angle α encountering a convected disturbance. Disturbance lengthscale λ is assumed to be much smaller than the airfoil chord.

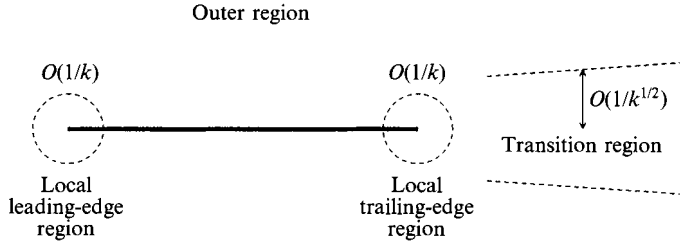

FIGURE 2. Illustration of asymptotic regions, with sizes given in dimensionless coordinates.

so small that this assumption is violated probably do not contribute much to the sound field. For $\alpha^2 k \ll 1$, the mean-flow gradients are weak when expressed in local leading-edge coordinates. This property is utilized in developing the solution in the leading-edge region.

In the analysis that follows, perturbation terms of relative order $k^{-1/2}$ and $\alpha k^{1/2}$ are retained, while those of relative order $1/k$, α, and $\alpha^2 k$ are neglected. If we set $k = O(\alpha^{-\gamma})$, this ordering is consistent with values of γ in the range $2/3 < \gamma < 2$.

The following sections present the details of the analysis in the various regions. Throughout the paper, upper-case letters are used for local (leading- or trailing-edge) quantities and lower-case letters for outer quantities. The unsubscripted independent variables are referenced from the leading edge. Additional subscripted variables, both dependent and independent, are defined in the course of the analysis.

3.1. *Local leading-edge region*

In the local leading-edge region, we introduce local coordinates (Φ, Ψ) which scale on the disturbance wavelength and have their origin at the leading edge. After choosing the arbitrary constant in (3.1*a*) to be $-i\pi$ (so that the drift function vanishes at upstream infinity), and substituting the coordinates

$$\Phi = k\phi, \quad \Psi = k\psi \tag{3.2}$$

into (3.1), we obtain the expansion

$$F = \frac{2^{3/2}}{k^{1/2}\beta_\infty}(\Phi + i\Psi)^{1/2} + O(1/k). \tag{3.3}$$

Hence, the mean-flow disturbance in this local region is dominated by the flow around the edge. It is interesting to note that the Drift function (2.5*d*), representing cumulative

phase distortion of the convected disturbances from upstream infinity, vanishes to $O(\alpha)$ at the leading edge. Upon utilizing the local expansion (3.3) in (2.4)–(2.6), we find that the solution in the leading-edge region has the asymptotic expansion

$$H_l = \frac{1}{k}[H_0 + \alpha k^{1/2}(H_1 + H_2 + H_3) + O(\alpha^2 k, \alpha)]. \tag{3.4}$$

The terms H_1, H_2 and H_3 are of equal importance, but have been separated because they represent different physical effects. The function H_1 represents the influence on the airfoil-surface boundary condition of vorticity distortion by mean-flow gradients, while H_2 is generated by the volume-source term of (2.4*b*) and H_3 contains the influence of local mean-flow gradients on the acoustic-propagation characteristics of the medium.

The solutions in the local leading-edge region are developed using Fourier-transform methods. In leading-edge coordinates the airfoil body appears semi-infinite. Hence the mixed boundary-value problems governing the functions in (3.4) may be solved by application of the Wiener–Hopf technique (Noble 1958). Our interest is in the sound which propagates to the far field, and for this only the asymptotic behaviour of these local solutions many wavelengths from the leading edge is required. This asymptotic behaviour is found by the method of steepest descent. The solutions for H_0, H_1, H_2 and H_3 are presented in the following subsections.

3.1.1. *Solution for* H_0

The first term H_0 is the classical leading-edge solution for the case of zero incidence angle. Here the sound generation is due solely to blocking by the airfoil surface of the undistorted vortical velocity. The governing equations are

$$\mathrm{L}(H_0) = 0 \tag{3.5a}$$

and

$$\left.\frac{\partial H_0}{\partial \Psi}\right|_{\Psi=0,\,\Phi>0} = -\frac{A_n}{\beta_\infty} e^{i\delta\Phi}, \tag{3.5b}$$

where

$$\mathrm{L} = \frac{\partial^2}{\partial \Phi^2} + \frac{\partial^2}{\partial \Psi^2} + w^2. \tag{3.5c}$$

Since the airfoil appears locally semi-infinite, the boundary condition is applied on the half-plane $\Phi > 0$. The solution

$$H_0 = -\frac{A_n \operatorname{sgn}(\Psi)}{\beta_\infty 2\pi(\delta + w)^{1/2}} \int_{-\infty}^{\infty} \frac{e^{a(\lambda, \Phi, \Psi)}\, d\lambda}{(\lambda + \delta)(\lambda + w)^{1/2}}, \tag{3.6a}$$

where

$$a(\lambda, \Phi, \Psi) = -i\lambda\Phi - |\Psi|(\lambda^2 - w^2)^{1/2} \tag{3.6b}$$

is found by a standard application of the Wiener–Hopf technique. The singularities of the integrand are a pole at $\lambda = -\delta$ and branch points at $\lambda = \pm w$. The pole corresponds to local hydrodynamic motion near the plate, while the branch points are related to acoustic motion. We take the inversion contour to be the real axis, and assume that δ and w have small positive imaginary parts. The singularities and associated branch cuts are shown on figure 3. (Additional singularities and branch cuts which arise later are also illustrated.)

The asymptotic matching with the outer solution requires the expansion of (3.6) in outer coordinates. For convenience we introduce polar forms of the inner coordinates,

$$R = (\Phi^2 + \Psi^2)^{1/2}, \quad \theta = \arctan(\Psi/\Phi), \tag{3.7a}$$

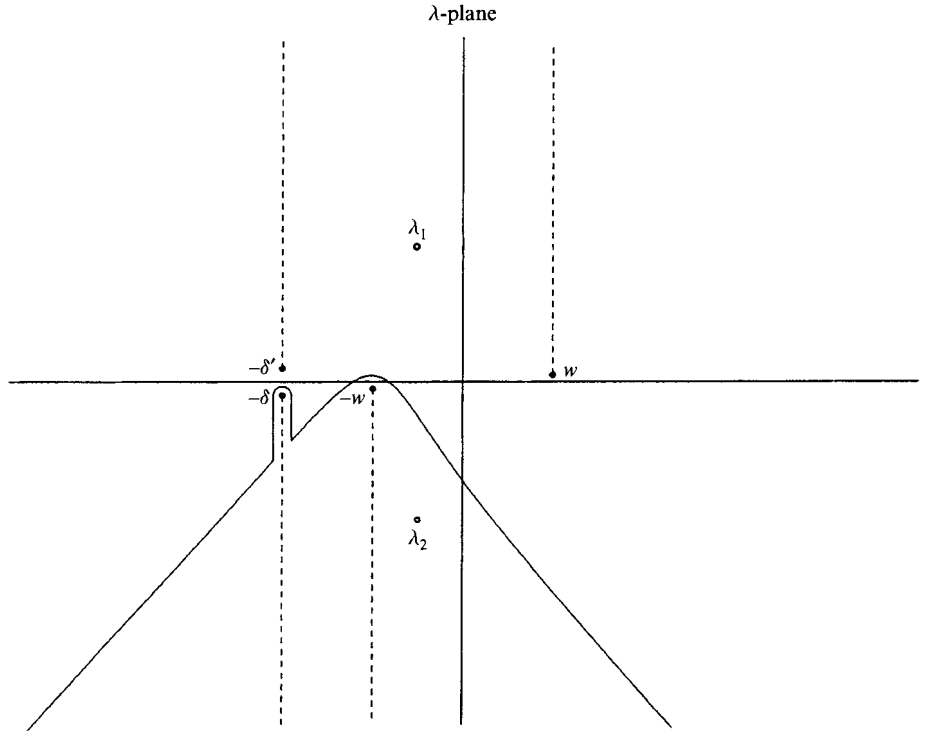

FIGURE 3. Singularities in the complex plane encountered at various stages of the analysis. (Branch cuts denoted by dashed lines.) Steepest descent path is also shown (solid curve.)

and the outer coordinates,

$$r = (\phi^2+\psi^2)^{1/2} = R/k, \quad \theta = \arctan(\psi/\phi) = \arctan(\Psi/\Phi). \tag{3.7b}$$

Inserting (3.7*b*) into (3.6) introduces the large parameter k in the exponent (3.6*b*), and the method of steepest descent can be utilized to obtain the asymptotic expansion. After a transformation to the steepest-descent path illustrated in figure 3, the integrand is dominated by points near the saddle point of $a(\lambda)$ at $\lambda_0 = -w\cos\theta$, and the method of steepest descent produces the expansion

$$H_0 = D_0(\theta)\frac{e^{ikwr}}{(kr)^{1/2}} + O(k^{-3/2}), \tag{3.8a}$$

where

$$D_0(\theta) = -\frac{A_n e^{-i\pi/4}\cos\frac{1}{2}\theta}{\beta_\infty[\pi(\delta+w)]^{1/2}(\delta-w\cos\theta)}. \tag{3.8b}$$

3.1.2. *Solution for* H_1

The function H_1 accounts for the $O(\alpha k^{1/2})$ terms in the local leading-edge expansion of the airfoil-surface boundary condition (2.6) which involve vorticity distortion. The governing equations are

$$L(H_1) = 0 \tag{3.9a}$$

and

$$\left.\frac{\partial H_1}{\partial \Psi}\right|_{\Psi=0^{\pm},\,\Phi>0} = \pm i4\sqrt{2}\,A_n\,\delta\Phi^{1/2}e^{i\delta\Phi}. \tag{3.9b}$$

The boundary condition arises from the local expansion of the drift function (2.5*d*) appearing in the phase Ω of the vortical velocity v'. Essentially, the local flow around

the leading edge increases the convection speed of the vorticity along the upper surface, and decreases it along the lower surface. Only the component of vortical velocity normal to the streamlines at upstream infinity appears in (3.9*b*), and the entropy disturbance does not enter. Note that the boundary condition (3.9*b*) corresponds to a source distribution rather than a vortex distribution as in (3.5*b*). Hence, H_1 is a symmetric function of Ψ, and a straightforward application of Fourier-transform methods leads to

$$H_1 = A_n \delta \frac{\sqrt{2}\,e^{i\pi/4}}{\pi^{1/2}} \int_{-\infty}^{\infty} \frac{e^{a(\lambda,\Phi,\Psi)}\,d\lambda}{(\lambda+\delta)^{3/2}(\lambda^2-w^2)^{1/2}}, \tag{3.10}$$

where δ is assumed to have a small positive imaginary part, ensuring convergence of the transform of (3.9*b*), and the branch point from $-\delta$ is taken in the lower half of the λ-plane. By introducing outer variables in (3.10) and again employing the method of steepest descent, we obtain the asymptotic expansion

$$H_1 = D_1(\theta)\frac{e^{ikwr}}{(kr)^{1/2}} + O(k^{-3/2}), \tag{3.11a}$$

where

$$D_1(\theta) = \frac{i2\,A_n\,\delta}{w^{1/2}(\delta - w\cos\theta)^{3/2}}. \tag{3.11b}$$

3.1.3. *Solution for* H_2

The function H_2 is generated by the volume-source term in (2.4*b*), which is $O(\alpha k^{1/2})$ in the local leading-edge region. The expansion of this source term in local leading-edge coordinates leads to the inhomogeneous differential equation

$$L(H_2) = e^{i(\delta\Phi + k_n\Psi)}\{R^{-1/2}[C_1\cos\tfrac{1}{2}\theta + C_2\sin\tfrac{1}{2}\theta] + R^{-3/2}[C_3\cos\tfrac{3}{2}\theta + C_4\sin\tfrac{3}{2}\theta]\}, \tag{3.12a}$$

where

$$\left.\begin{aligned} C_1 &= i2^{3/2}\left(\frac{\delta A_t^*}{\beta_\infty} - k_n A_n\right), \quad C_3 = -\frac{\sqrt{2}\,A_t^* M_\infty^2}{\beta_\infty^3}, \\ C_2 &= i2^{3/2}\left(\frac{k_n A_t^*}{\beta_\infty} + \delta A_n\right), \quad C_4 = -\frac{\sqrt{2}\,A_n M_\infty^2}{\beta_\infty^2}. \end{aligned}\right\} \tag{3.12b}$$

The source term in (3.12*a*) is closely related to the quadrupole source of Ffowcs Williams & Hawkings (1969*b*). We choose to satisfy the boundary condition

$$\left.\frac{\partial H_2}{\partial \Psi}\right|_{\Psi=0,\,\Phi>0} = 0, \tag{3.12c}$$

and hence H_2 is also related to the quadrupole field scattered by the leading edge as discussed by Ffowcs Williams & Hall (1970). The exact correspondence between our work and that of these authors is discussed later.

A particular solution for H_2 is obtained by applying a double Fourier transform to (3.12*a*), followed by inversion on Ψ through contour integration. The result is

$$H_{2p} = \frac{e^{i\pi/4}}{8\pi^{1/2}(\delta^2+k_n^2)}\left\{e^{ik_n\Psi}\int_{-\infty}^{\infty}\left[\frac{f_1(\lambda)}{(\lambda+\delta')^{1/2}} - \frac{\operatorname{sgn}(\Psi)f_2(\lambda)}{(\lambda+\delta)^{1/2}}\right]\frac{e^{hy(\lambda,\Phi,\Psi)}\,d\lambda}{(\lambda-\lambda_1)(\lambda-\lambda_2)}\right.$$
$$\left. - \int_{-\infty}^{\infty}\left[\frac{(\lambda+\delta)f_1(\lambda) + ik_n f_2(\lambda)}{(\lambda^2-w^2)^{1/2}} - \operatorname{sgn}(\Psi)f_2(\lambda)\right]\frac{e^{a(\lambda,\Phi,\Psi)}\,d\lambda}{(\lambda+\delta)^{1/2}(\lambda-\lambda_1)(\lambda-\lambda_2)}\right\}, \tag{3.13a}$$

where

$$hy(\lambda,\Phi,\Psi) = -i\lambda\Phi - |\Psi|[(\lambda+\delta)(\lambda+\delta')]^{1/2}, \tag{3.13b}$$

$$f_1(\lambda) = [\mathrm{i}C_2 - 2C_4(\lambda+\delta)](-\delta^2+k_n^2-w^2-2\delta\lambda)+[C_1+2\mathrm{i}C_3(\lambda+\delta)]\,2\mathrm{i}k_n(\lambda+\delta), \tag{3.13c}$$

$$f_2(\lambda) = [\mathrm{i}C_2 - 2C_4(\lambda+\delta)]\,2\mathrm{i}k_n(\lambda+\delta)+[C_1+2\mathrm{i}C_3(\lambda+\delta)](-\delta^2+k_n^2-w^2-2\delta\lambda), \tag{3.13d}$$

and

$$\lambda_{1,2} = -\frac{\delta}{2}\left[\frac{\delta^2+k_n^2+w^2}{\delta^2+k_n^2}\right] \pm \frac{\mathrm{i}k_n}{2}\left[\frac{\delta^2+k_n^2-w^2}{\delta^2+k_n^2}\right]. \tag{3.13e}$$

Here δ' is assumed to have a small negative imaginary part as contrasted to the small positive imaginary part in δ. The poles and branch points contained in (3.13*a*) are shown in figure 3. The phase $hy(\lambda, \Phi, \Psi)$ is 'hydrodynamic' as opposed to the 'acoustic' phase $a(\lambda, \Phi, \Psi)$ defined earlier in (3.6*b*). For large R, integrals containing $hy(\lambda, \Phi, \Psi)$ represent disturbances which are convected by the mean flow, while integrals containing $a(\lambda, \Phi, \Psi)$ represent disturbances which propagate at the speed of sound relative to the mean flow. The functions f_1 and f_2 are quadratic functions of their arguments whose coefficients depend on the gust characteristics and mean-flow Mach number.

The second integral in H_{2p}, with the phase $a(\lambda, \Phi, \Psi)$, actually satisfies the homogeneous equation $\mathrm{L}(H) = 0$. This contribution arises naturally in the utilization of Fourier transforms and is essential for the solution to obey the correct edge condition near the airfoil leading edge. In the absence of this contribution the particular solution asymptotically behaves as $R^{-1/2}$ near the leading edge, while with it the behaviour is $R^{1/2}$. A direct integration of the source term in (3.12*a*) in the $R \ll 1$ limit confirms that the solution H_2 should exhibit $R^{1/2}$ behaviour near the leading edge.

Contour integration shows that the particular solution H_{2p} and its derivative $\partial H_{2p}/\partial\Psi$ are continuous across the line $\Psi = 0$, but $\partial H_{2p}/\partial\Psi$ is non-zero for $\Phi > 0$. Hence, a complementary solution H_{2c} is required in order to satisfy (3.12*c*). The calculation of H_{2c} involves a non-standard application of the Wiener–Hopf technique, which is presented in the Appendix. The result is

$$H_{2c} = -\frac{\mathrm{sgn}(\Psi)\,\mathrm{e}^{\mathrm{i}\pi/4}}{8\pi^{1/2}(\delta^2+k_n^2)}\int_{-\infty}^{\infty}\left[4\mathrm{i}k_n\,C_4+4\mathrm{i}\delta C_3-\frac{(\lambda_1+w)^{1/2}f_2(\lambda_1)}{(\lambda_1-\lambda_2)(\lambda_1+\delta)^{1/2}(\lambda-\lambda_1)}\right.$$
$$\left.+\frac{(\lambda_2+\delta)f_2(\lambda_2)+\mathrm{i}k_n f_1(\lambda_2)}{[(\lambda_2-w)(\lambda_2+\delta')]^{1/2}(\lambda_1-\lambda_2)(\lambda-\lambda_2)}+\frac{(\lambda+w)^{1/2}f_2(\lambda)}{(\lambda+\delta)^{1/2}(\lambda-\lambda_1)(\lambda-\lambda_2)}\right]\frac{\mathrm{e}^{a(\lambda,\Phi,\Psi)}\,\mathrm{d}\lambda}{(\lambda+w)^{1/2}}. \tag{3.14}$$

In order to match with the outer solution developed in the next section, we expand H_2 in outer variables. The integrals containing the acoustic phase $a(\lambda, \Phi, \Psi)$ are expanded asymptotically by the method of steepest descent as discussed previously. The only complication is the path deformations required around the branch cuts emanating from δ and δ'. It can be shown that the contributions from the vicinities of these branch points are exponentially small compared to that arising from the saddle point of $a(\lambda, \Phi, \Psi)$. For the integrals containing the phase $hy(\lambda, \Phi, \Psi)$, the integration path along the real axis is deformed into two rays which meet on the real axis at $\lambda = -\delta$, and along which the imaginary part of $hy(\lambda, \Phi, \Psi)$ is constant. (Deformations are required around the branch cuts emanating from $\pm w$.) The integrand is exponentially decaying along the rays and the dominant contribution comes from the vicinity of $\lambda = -\delta$. The asymptotic expansions are given by

$$H_{2p} = \frac{\mathrm{e}^{\mathrm{i}k(\delta\phi+k_n\psi)}}{(\delta^2+k_n^2-w^2)(kr)^{1/2}}[C_1\cos\tfrac{1}{2}\theta + C_2\sin\tfrac{1}{2}\theta] + D_{2p}(\theta)\frac{\mathrm{e}^{\mathrm{i}kwr}}{(kr)^{1/2}} + O(k^{-3/2}) \tag{3.15a}$$

with $$D_{2p}(\theta) = \frac{-\mathrm{i}(\delta - w\cos\theta) f_1(-w\cos\theta) + k_n f_2(-w\cos\theta)}{4(\delta^2 + k_n^2)\,[2w(\delta - w\cos\theta)]^{1/2}(\lambda_1 + w\cos\theta)\,(\lambda_2 + w\cos\theta)}, \tag{3.15b}$$

and $$H_{2c} = D_{2c}(\theta)\frac{\mathrm{e}^{\mathrm{i}kwr}}{(kr)^{1/2}} + O(k^{-3/2}) \tag{3.15c}$$

with

$$D_{2c}(\theta) = -\left[4(\lambda_1 - \lambda_2)(\mathrm{i}k_n C_4 + \mathrm{i}\delta C_3) + \frac{(\lambda_1 + w)^{1/2} f_2(\lambda_1)}{(\lambda_1 + \delta)^{1/2}(\lambda_1 + w\cos\theta)} - \frac{(\lambda_2 + \delta) f_2(\lambda_2) + \mathrm{i}k_n f_1(\lambda_2)}{[(\lambda_2 - w)(\lambda_2 + \delta')]^{1/2}(\lambda_2 + w\cos\theta)}\right] \frac{\cos\frac{1}{2}\theta}{4(\lambda_1 - \lambda_2)(\delta^2 + k_n^2)}. \tag{3.15d}$$

The first term of (3.15*a*) arises from the integral in H_{2p} containing $hy(\lambda, \Phi, \Psi)$, and represents a disturbance convected at the mean-flow speed. The other terms in (3.15) arise from the integrands containing $a(\lambda, \Phi, \Psi)$, and represent sound generated by the volume quadrupoles and the subsequent scattering by the leading edge. For compactness in later expressions for the outer acoustic field, we combine the volume-source-related directivities D_{2p} and D_{2c}:

$$D_2(\theta) = D_{2p}(\theta) + D_{2c}(\theta). \tag{3.15e}$$

3.1.4. *Solution for H_3*

The function H_3 represents the influence, in the local leading-edge region, of the spatial variation of the coefficients in the wave operator of (2.1*b*). The spatial variation of the coefficients is related to sound propagation through a variable-property medium. In the local leading-edge region, the spatial variation of the medium occurs on the same scale as the acoustic wavelength, and hence the interaction of the acoustic field with these local gradients can result in additional sound radiation to the far field.

In our simplified wave equation (2.4*b*) for a small-perturbation mean flow, the variable coefficients are contained in the operator L_1. Upon using (3.1*b*) to express (2.4*d*) in local leading-edge coordinates, and substituting the expansion (3.4) into (2.4*b*), we find that $\alpha \mathrm{L}_1(H_0)$ becomes an $O(\alpha k^{1/2})$ contribution which can be taken over to the right-hand side as a source term. The resulting inhomogeneous equation is

$$\mathrm{L}(H_3) = \frac{\sqrt{2}}{\beta_\infty} R^{-1/2}\cos\tfrac{1}{2}\theta \left\{2\beta_\infty^2 w^2 H_0 - (\gamma+1)\frac{M_\infty^4}{\beta_\infty^2} \times \left[\frac{\partial^2 H_0}{\partial \Psi^2} + 2\mathrm{i}\delta\frac{\partial H_0}{\partial \Phi} + (w^2 + \delta^2) H_0\right]\right\} - R^{-3/2}\cos\tfrac{3}{2}\theta \frac{(\gamma+1) M_\infty^4}{\sqrt{2}\,\beta_\infty^3}\left[\frac{\partial H_0}{\partial \Phi} - \mathrm{i}\delta H_0\right]. \tag{3.16a}$$

The applicable boundary condition is the $O(\alpha k^{1/2})$ term in the local expansion of (2.6), minus the contribution contained in (3.9*b*) representing vorticity distortion. The remainder, which represents a shift of spatial gradients from the original wave operator to the boundary condition by the transformation (2.4*a*), is

$$\left.\frac{\partial H_3}{\partial \Psi}\right|_{\Psi = 0^{\pm},\, \Phi > 0} = \pm\sqrt{2}\, A_n \frac{M_\infty^2}{\beta_\infty^2} \Phi^{-1/2}\, \mathrm{e}^{\mathrm{i}\delta\Phi}. \tag{3.16b}$$

The function H_0 appearing in the source terms of (3.16*a*) is known only in the

Fourier-integral form (3.6). However, note that the source terms are products of harmonic functions with solutions of the Helmholtz equation $\mathrm{L}(H) = 0$. This property can be exploited to determine a particular solution in the following way. First we evaluate the derivatives of H_0 appearing in the source terms by differentiating under the integral sign. Next consider a function of the form

$$F(\Phi, \Psi) = f(\Phi, \Psi) \int_{-\infty}^{\infty} C(\lambda)\, \mathrm{e}^{a(\lambda, \Phi, \Psi)}\, \mathrm{d}\lambda, \tag{3.17}$$

where f is harmonic and a is given by (3.6*b*). Application of the operator L to this function yields

$$\mathrm{L}(F) = -2\left[\mathrm{i}\frac{\partial f}{\partial \Phi}\int_{-\infty}^{\infty} \lambda C(\lambda)\, \mathrm{e}^{a(\lambda, \Phi, \Psi)}\, \mathrm{d}\lambda + \operatorname{sgn}(\Psi) \times \frac{\partial f}{\partial \Psi}\int_{-\infty}^{\infty} (\lambda^2 - w^2)^{1/2} C(\lambda)\, \mathrm{e}^{a(\lambda, \Phi, \Psi)}\, \mathrm{d}\lambda\right] \tag{3.18}$$

in regions where the functions involved are continuous. A particular solution to (3.16*a*) can be obtained by proper combinations of choices for the functions $f(\Phi, \Psi)$ and $C(\lambda)$.

To find a particular solution for the source terms containing $R^{-1/2}\cos\frac{1}{2}\theta$, we utilize the functions

$$f_1 = R^{1/2}\cos\tfrac{1}{2}\theta \quad \text{and} \quad f_2 = R^{1/2}\sin\tfrac{1}{2}\theta. \tag{3.19a, b}$$

After substituting (3.19) into (3.18) and equating the coefficients under the integral sign with the corresponding coefficients in the source terms of (3.16*a*), we possess a set of linear algebraic equations for the coefficients $C_1(\lambda)$ and $C_2(\lambda)$. A similar procedure is utilized for the source terms containing $R^{-3/2}\cos\frac{3}{2}\theta$. The final result can be written in terms of derivatives of H_0, as

$$\begin{aligned} H_{3p} = {} & R^{1/2}\left(\cos\tfrac{1}{2}\theta\frac{\partial}{\partial\Phi} + \sin\tfrac{1}{2}\theta\frac{\partial}{\partial\Psi}\right)\left[\left(\frac{\partial^2}{\partial\Psi^2} + 2\mathrm{i}\delta\frac{\partial}{\partial\Phi} + w^2 + \delta^2\right)\right. \\ & \left.\times\frac{\sqrt{2(\gamma+1)}\, M_\infty^4 H_0}{\beta_\infty^3 w^2} - 2^{3/2}\beta_\infty H_0\right] + \tfrac{1}{2}R^{-1/2}\left(-\cos\tfrac{1}{2}\theta\frac{\partial}{\partial\Phi} + \sin\tfrac{1}{2}\theta\frac{\partial}{\partial\Psi}\right) \\ & \times\left(\frac{\partial}{\partial\Phi} - \mathrm{i}\delta\right)\frac{\sqrt{2(\gamma+1)}\, M_\infty^4 H_0}{\beta_\infty^3 w^2}. \end{aligned} \tag{3.20}$$

This particular solution and its derivatives are continuous across $\Psi = 0$ in front of the airfoil ($\Phi < 0$), but on the airfoil surface contour integration produces

$$\left.\frac{\partial H_{3p}}{\partial\Psi}\right|_{\Psi=0^{\pm},\, \Phi>0} = \pm\sqrt{2}\, A_n\left[2\mathrm{i}\delta\Phi^{1/2} + \Phi^{-1/2}\right]\mathrm{e}^{\mathrm{i}\delta\Phi}. \tag{3.21}$$

This expression must be combined with (3.16*b*) to form the boundary condition for a complementary function H_{3c}. Direct Fourier transformation yields the complementary solution

$$H_{3c} = A_n\frac{\mathrm{e}^{\mathrm{i}\pi/4}}{(2\pi)^{1/2}}\int_{-\infty}^{\infty}\left[\frac{1 - M_\infty^2/\beta_\infty^2}{(\lambda+\delta)^{1/2}} - \frac{\delta}{(\lambda+\delta)^{3/2}}\right]\frac{\mathrm{e}^{a(\lambda,\phi,\Psi)}}{(\lambda^2 - w^2)^{1/2}}\,\mathrm{d}\lambda. \tag{3.22}$$

One additional modification is required to complete the solution for H_3. The

combination of H_{3p} and H_{3c} satisfies the differential equation and boundary condition, but H_{3p} exhibits unacceptable singular behaviour near the origin. A local analysis for $R \ll 1$ shows that the particular solution given by (3.20) behaves as

$$\frac{2^{3/2} A_n \, e^{i\pi/4}}{\pi^{1/2}(\delta+w)^{1/2}} + \frac{\sqrt{2}\, A_n \, e^{i\pi/4}(\gamma+1) M_\infty^4}{\pi^{1/2}\beta_\infty^4(\delta+w)^{1/2}} \left\{ \left[-\frac{\cos 2\theta}{2w^2R^2}\left(1+\frac{w^2R^2}{4}\right) - \frac{i\delta\cos\theta}{2w^2R} \right] + \frac{1}{4} - \frac{\delta}{2w} + \frac{\cos 2\theta}{8} + \frac{\cos\theta}{2} \right\} + O(R^{1/2}). \quad (3.23)$$

The portion of (3.23) in square brackets is a local expansion of spurious eigensolutions of the differential operator (3.5*c*), with zero-normal-derivative boundary condition on the plate surface. The eigensolutions are presumably introduced by the multiple differentiations utilized to derive (3.20). The remainder of (3.23) is consistent with a direct local integration of the source term in (3.16*a*). Thus, the singular behaviour of (3.23) must be removed by adding eigensolutions of the appropriate sign to (3.20), bringing the small-R dependence of the particular solution to that predicted by a direct local integration of the source term. Hence we set

$$H_3 = H_{3p} + H_{3c} + H_{3e}, \quad (3.24)$$

where

$$H_{3e} = \frac{-\sqrt{2}(\gamma+1) M_\infty^4 A_n \, e^{-i\pi/4} \pi^{1/2}}{8\beta_\infty^4(\delta+w)^{1/2}} \left(H_2^{(1)}(wR)\cos 2\theta + \frac{2i\delta}{w} H_1^{(1)}(wR)\cos\theta \right) \quad (3.25)$$

and $H_1^{(1)}$ and $H_2^{(1)}$ denote first-order and second-order Hankel functions of the first kind (Abramowitz & Stegun 1972).

For asymptotic matching with the outer region, the expansion of H_3 in outer coordinates is required. Expansion of (3.20) requires only the use of expansion (3.8) for H_0, while solutions (3.22) and (3.25) can be expanded using the method of steepest descent and the known expansions for the Hankel functions. The results are

$$H_{3p} = [i(2kr)^{1/2}w] \left[-2\beta_\infty + \frac{(\gamma+1) M_\infty^4}{\beta_\infty^3 w^2} (\delta - w\cos\theta)^2 \right] (\cos\tfrac{1}{2}\theta) H_0 + O(k^{-1}), \quad (3.26a)$$

where H_0 represents (3.8), and

$$H_{3c} + H_{3e} = D_3(\theta) \frac{e^{ikwr}}{(kr)^{1/2}} + O(k^{-3/2}), \quad (3.26b)$$

where

$$D_3(\theta) = \frac{iA_n}{[w(\delta - w\cos\theta)]^{1/2}} \left[1 - \frac{M_\infty^2}{\beta_\infty^2} - \frac{\delta}{\delta - w\cos\theta} \right] + \frac{iA_n(\gamma+1) M_\infty^4}{w^{3/2}(\delta+w)^{1/2}\beta_\infty^4} \left[\frac{\delta}{2}\cos\theta - \frac{w}{4}\cos 2\theta \right]. \quad (3.26c)$$

The first and second parts of (3.26*c*) come from H_{3c} and H_{3e}, respectively. Note that the asymptotic expansion (3.26*a*) of H_{3p} is singular with respect to H_0, indicating the need for a different expansion at larger distances from the leading edge (when $R = O(k)$).

This completes the solution for the $O(\alpha k^{1/2})$ correction to the unsteady motion in the local leading-edge region. Many effects not present for an airfoil at zero incidence

appear at this stage of the analysis. These include modifications to the boundary condition on the airfoil surface, volume-source terms related to the interaction of the convected disturbances with mean-flow gradients, and the influence of spatial variations in the acoustic properties of the medium. To understand how these effects propagate to the far field, we next analyse the outer region.

3.2. *Outer region*

In the outer region, the mean flow varies on the lengthscale of the airfoil chord, and hence (2.4*b*) is the appropriate non-dimensional form of the governing equation. Since the wavelength of the unsteady disturbance is small compared to the airfoil chord, we anticipate multiple-scales-type solutions in this region.

It is convenient to separate the solution in the outer region into four components. The first component h_p is a particular solution that accounts for the volume-source term in (2.4*b*), while the second component h_c is a complementary solution required to satisfy the boundary condition on the airfoil surface. In addition, the asymptotic matching of the outer solution with the local leading-edge and trailing-edge regions requires the introduction of two-additional components h_l and h_t. Thus we set

$$h = h_p + h_c + h_l + h_t. \tag{3.27}$$

We first solve for h_p. In the source term of (2.4*b*) the phase $k\Omega$ varies rapidly compared to the amplitude $S(\phi, \psi)$. Hence it is natural to seek a particular solution which also contains this rapidly varying phase. By utilizing the fact that derivatives with respect to the phase dominate those with respect to the amplitude, the particular solution

$$h_p = \frac{\alpha}{k} \frac{S(\phi, \psi)\, \mathrm{e}^{\mathrm{i}k\Omega}}{[w^2 - \delta^2 - k_n^2]} + O(\alpha^2/k, \alpha/k^2) \tag{3.28}$$

is readily found. The $O(1/k)$ terms in $S(\phi, \psi)$ can be neglected in (3.28).

The particular solution h_p does not satisfy the boundary condition (2.6) on the airfoil surface. Thus a complementary solution h_c is required. The complementary solution is exponentially small outside thin layers $\psi = O(1/k)$ adjacent to the airfoil surfaces. To account for this boundary-layer behaviour, we express h_c as a function of ϕ and Ψ. By again taking advantage of the rapidly varying phase $k\Omega$, occurring in the normal derivative of (3.28) as well as in the right-hand side of (2.6), we derive the following complementary solution for the outer region:

$$h_c(\phi, \Psi) = \frac{\operatorname{sgn}(\Psi)}{k} \frac{J_\pm(\phi)}{j_\pm(\phi)} \mathrm{e}^{-j_\pm(\phi)|\Psi|}\, \mathrm{e}^{\mathrm{i}k\Omega(\phi, 0^\pm)} + O(\alpha^2/k, \alpha/k^2), \tag{3.29a}$$

where

$$J_\pm(\phi) = \frac{A_n}{\beta_\infty}(1 - \alpha M_\infty^2\, q(\phi, 0^\pm)) + \alpha \frac{2A_t^*}{\beta_\infty} + \alpha \frac{\mathrm{i}k_n\, S(\phi, 0^\pm)}{w^2 - \delta^2 - k_n^2} \tag{3.29b}$$

and

$$j_\pm(\phi) = (\delta^2 - w^2)^{1/2} + \alpha \frac{w^2\beta^2 - 2\delta}{(\delta^2 - w^2)^{1/2}} q(\phi, 0^\pm). \tag{3.29c}$$

The general characteristics of h_p and h_c are similar. Both contain the phase $k\Omega$, which also appears in the vortical velocity v'. Thus, although the disturbances corresponding to h_p and h_c are irrotational, these disturbances convect with the mean flow and are not sound waves. The velocity fluctuations produced by h_p are $O(\alpha)$, while

the velocity fluctuations associated with h_c have $O(1)$ and $O(\alpha)$ components. In contrast, the pressure fluctuations for both h_p and h_c are only $O(\alpha/k)$, since the expression for pressure involves a substantial derivative. Hence only derivatives of the slowly varying amplitudes contribute to the pressure field. This result is not surprising, since linear disturbances convected by a uniform flow produce no pressure fluctuations.

The third component of the outer solution, h_l, corresponds to propagating acoustic waves generated at the airfoil leading edge. This solution is developed in the following subsection.

3.2.1. *Leading-edge ray field*

For the leading-edge ray field, the homogeneous form of the wave equation (2.4*b*) applies, along with a matching requirement with the local leading-edge region and the radiation condition at infinity. We utilize the polar form (r, θ) of the outer coordinates (ϕ, ψ), with $r = 0$ corresponding to the airfoil leading edge. After substituting the geometric-acoustics form

$$h_l = k^{-3/2} A_l(r, \theta)\, \mathrm{e}^{\mathrm{i}k\sigma_l(r,\theta)} + O(k^{-5/2}) \tag{3.30}$$

into (2.4*b*) and separating orders of k (the factor $k^{-3/2}$ has been introduced in anticipation of the asymptotic matching) we obtain the eikonal equation

$$\left(\frac{\partial\sigma_l}{\partial r}\right)^2 + \frac{1}{r^2}\left(\frac{\partial\sigma_l}{\partial\theta}\right)^2 - w^2 + \alpha q\left\{2w^2\beta_\infty^2 + \frac{(\gamma+1)M_\infty^4}{\beta_\infty^2} \times\left[\left(\sin\theta\frac{\partial\sigma_l}{\partial r} + \frac{\cos\theta}{r}\frac{\partial\sigma_l}{\partial\theta}\right)^2 + 2\delta\left(\cos\theta\frac{\partial\sigma_l}{\partial r} - \frac{\sin\theta}{r}\frac{\partial\sigma_l}{\partial\theta}\right) - \delta^2 - w^2\right]\right\} + O(\alpha^2) = 0 \tag{3.31}$$

and the transport equation

$$\frac{\partial\sigma_l}{\partial r}\frac{\partial A_l}{\partial r} + \frac{1}{r}\frac{\partial\sigma_l}{\partial\theta}\frac{\partial A_l}{\partial\theta} + \frac{A_l}{2}\left[\frac{1}{r}\frac{\partial}{\partial r}\left(r\frac{\partial\sigma_l}{\partial r}\right) + \frac{1}{r^2}\frac{\partial^2\sigma_l}{\partial\theta^2}\right] + O(\alpha) = 0. \tag{3.32}$$

We seek a solution for the eikonal equation in the form of a perturbation series

$$\sigma_l = \sigma_{0l} + \alpha\sigma_{1l} + O(\alpha^2), \tag{3.33}$$

where the leading term

$$\sigma_{0l} = wr \tag{3.34}$$

is the cylindrical-wave phase appropriate for a flat plate at zero incidence. The first-order correction σ_{1l} to the phase then satisfies

$$\frac{\partial\sigma_{1l}}{\partial r} = qV(\theta), \tag{3.35a}$$

where

$$V(\theta) = -\beta_\infty^2 w + \frac{(\gamma+1)M_\infty^4}{2\beta_\infty^2 w}(\delta - w\cos\theta)^2. \tag{3.35b}$$

We take advantage of the fact that $q(\phi, \psi)$ is the real part of an analytic function $\mathrm{d}F/\mathrm{d}\zeta$ and integrate (3.35*a*) in the form

$$\sigma_{1l} = V(\theta)\,\mathrm{Re}\,(\mathrm{e}^{-\mathrm{i}\theta}F(r\,\mathrm{e}^{\mathrm{i}\theta})) + g_{1l}(\theta). \tag{3.35c}$$

Here the perturbation complex potential F is given by (3.1*a*), with the arbitrary constant C chosen as $-\mathrm{i}\pi$ so that F vanishes at the leading edge. The function of integration g_{1l} will be determined by matching. Note that F is discontinuous across

$\psi = 0$, and hence σ_{1l} is discontinuous as well, owing to the differences in convection and sound speed above and below the airfoil. For matching with the local leading-edge region, the expansion

$$\sigma_{1l} \sim \frac{V(\theta)}{\beta_\infty} 2^{3/2} r^{1/2} \cos\tfrac{1}{2}\theta + g_{1l}(\theta) + O(r), \quad r \ll 1 \tag{3.35d}$$

is needed, while the expansion

$$\sigma_{1l} \sim \frac{V(\theta)}{\beta_\infty}[(1+\log 2r)\sin\theta + (\pi-\theta)\cos\theta] + g_{1l}(\theta) + O(1/r), \quad r \gg 1 \tag{3.35e}$$

is useful for determination of the far field. We neglect the $O(\alpha^2)$ correction to the phase σ_l, consistent with our neglect of $O(\alpha^2 k)$ terms in the solution for the local leading-edge region.

The solution of the transport equation (3.32) is simply given by

$$A_l = r^{-1/2} K_l(\theta) + O(\alpha), \tag{3.36}$$

where the neglect of $O(\alpha)$ amplitude terms is consistent with the neglect of $O(\alpha^2 k)$ terms arising from the phase.

We now utilize Van Dyke's (1975) rule to match the acoustic solutions in the local leading-edge region and the outer region. The two-term outer expansion of (3.4), contained in (3.8), (3.11), (3.15), and (3.26), must agree with the two-term local expansion of (3.30), when expressed in the same coordinates. The expansions are found to match if we set

$$K_l(\theta) = D(\theta) \equiv D_0(\theta) + \alpha k^{1/2}(D_1(\theta) + D_2(\theta) + D_3(\theta)) \tag{3.37a}$$

and

$$g_{1l}(\theta) = 0. \tag{3.37b}$$

Hence the directivities of the cylindrical waves emanating from the local leading-edge region appear without change of form in the outer region. Also, in the course of matching the singular expansion (3.26*a*) is seen to be recast as a geometric phase distortion σ_{1l} and an $O(1)$ amplitude ($= D_0(\theta)/r^{1/2}$) in the outer region.

The final component h_t of the solution in the outer region corresponds to acoustic waves generated at the airfoil trailing edge. Deferring for the moment the source of these waves, we next outline the derivation of the trailing-edge ray field.

3.2.2. *Trailing-edge ray field*

The trailing-edge ray field satisfies the same governing equation and radiation condition as the leading-edge ray field, and a matching condition with the local trailing-edge region. The functional form of the leading-edge ray solution may be used again, if reference is made to a new coordinate system (r_t, θ_t) originating at the trailing edge. Owing to the net circulation around the airfoil, the trailing edge is located at different values of the coordinate ϕ above and below the airfoil. The location of the trailing edge is given by $\phi = 2 \pm \alpha\pi/\beta_\infty$, where the plus and minus signs apply on the airfoil upper ($\psi = 0^+$) and lower ($\psi = 0^-$) surfaces, respectively. Thus, trailing-edge-based coordinates for the outer region are

$$\phi_t = \phi - (2 \pm \alpha\pi/\beta_\infty), \quad \psi_t = \psi, \tag{3.38a,b}$$

where the plus and minus signs in (3.38*a*) apply for $\psi \gtrless 0$, respectively. The coordinates (r_t, θ_t) are the polar form of (ϕ_t, ψ_t).

The trailing-edge ray field has the geometric-acoustics form

$$h_t = k^{-2} A_t(r_t, \theta_t)\, \mathrm{e}^{\mathrm{i}k\sigma_t(r_t,\theta_t)} + O(k^{-3}). \tag{3.39}$$

Analogously to (3.33), the phase is given by the asymptotic series

$$\sigma_t = w r_t + \alpha \sigma_{1t} + O(\alpha^2), \tag{3.40a}$$

where

$$\sigma_{1t} = \left[-\beta_\infty^2 w + \frac{(\gamma+1) M_\infty^4}{2\beta_\infty^2 w} (\delta - w\cos\theta_t)^2 \right] \int_0^{r_t} q(r_t', \theta_t)\, \mathrm{d}r_t' + g_{1t}(\theta_t) \tag{3.40b}$$

$$= V(\theta_t)\, \mathrm{Re}\{\mathrm{e}^{-\mathrm{i}\theta_t} F_t(r_t\, \mathrm{e}^{\mathrm{i}\theta_t})\} + g_{1t}(\theta_t). \tag{3.40c}$$

The function $F_t(\zeta_t)$ in (3.40c),

$$F_t(\zeta_t) = \frac{\mathrm{i}}{\beta_\infty} [\log\{\zeta_t + 1 + [\zeta_t(\zeta_t+2)]^{1/2}\} + \zeta_t - [\zeta_t(\zeta_t+2)]^{1/2}], \tag{3.41}$$

is the complex potential F in (3.1), expressed in trailing-edge coordinates $\zeta_t = \phi_t + \mathrm{i}\psi_t$, and with the arbitrary constant C chosen so that F_t vanishes at the trailing edge. The expansion of σ_{1t} for $r_t \gg 1$, to be utilized in the far-field solution, is

$$\sigma_{1t} \sim \frac{V(\theta_t)}{\beta_\infty} [-\theta_t \cos\theta_t + \sin\theta_t(-1 + \log 2r_t)] + g_{1t}(\theta_t) + O(1/r_t). \tag{3.42}$$

The trailing-edge phase distortion is discontinuous across $\psi = 0$ on the airfoil and in front of it, just as σ_{1l} was discontinuous on the airfoil and behind it.

The amplitude of the trailing-edge ray field is given by the following expression, similar to (3.36) in the leading-edge solution:

$$A_t = r_t^{-1/2} K_t(\theta_t) + O(\alpha). \tag{3.43}$$

$K_t(\theta_t)$ and $g_{1t}(\theta_t)$ are obtained by matching with the local trailing-edge region, which is discussed next.

3.3. *Local trailing-edge region*

In the local trailing-edge region we define coordinates which scale on the disturbance wavelength,

$$\Phi_t = k\phi_t, \quad \Psi_t = k\psi_t. \tag{3.44}$$

We begin our analysis of the local trailing-edge region by discussing the effect of the interaction of the convected disturbance with the trailing edge. Near the trailing edge, the steady Kutta condition results in a mean flow which locally is nearly uniform. Negligible ($O(\alpha)$) sound is therefore generated through distortion of the convected disturbance. The imposition of the unsteady Kutta condition at the trailing edge precludes sound generation by the discontinuity in boundary condition, because the vorticity shed into the wake is basically a continuation of the bound vorticity in the airfoil. Essentially, the convected singularities which cancel the gust velocity v' on the airfoil can be continued through the local trailing-edge region and extended to downstream infinity. The hydrodynamic solution (3.29) also applies throughout the local trailing-edge region and along the wake sheet ($\phi_t > 0$, $\psi_t = 0$) in the outer region.

In contrast to the convected disturbance, there are pressure fluctuations associated with the leading-edge ray-acoustic field. In general, the leading-edge ray field has different values above and below the airfoil. The difference in pressure at the trailing edge is cancelled by a local scattered field, which becomes the source of additional rays in the outer region.

The pressure associated with the leading-edge ray field is found by inserting the solution (3.30) into the expression (2.8) for the modified pressure. In the local trailing-edge region, the pressure jump across the wake is

$$p|_{\psi=0^-}^{\psi=0^+} = \frac{\Delta_p}{k^{1/2}} e^{i(w-\delta M_\infty^2)\Phi_t}, \tag{3.45a}$$

where

$$\Delta_p = \frac{i}{\sqrt{2}}(w-\delta)[D(0)\, e^{ik\sigma_l(2+\alpha\pi/\beta_\infty,\,0)}\, e^{-iC_+} - D(2\pi)\, e^{ik\sigma_l(2-\alpha\pi/\beta_\infty,\,2\pi)}\, e^{-iC_-}]. \tag{3.45b}$$

The function $D(\theta)$ is the local leading-edge directivity given by (3.37*a*), σ_l is the leading-edge phase function defined in (3.33)–(3.35), and the constants $C_\pm$ are defined by

$$C_\pm = k\delta M_\infty^2(2 \pm \alpha\pi/\beta_\infty). \tag{3.45c}$$

The local scattered field $H_t(\Phi_t, \Psi_t)$ which cancels this pressure jump is governed by the constant-coefficient Helmholtz equation, since non-uniform propagation effects are negligibly small in the local trailing-edge region. Thus,

$$\frac{\partial^2 H_t}{\partial \Phi_t^2} + \frac{\partial^2 H_t}{\partial \Psi_t^2} + w^2 H_t = 0. \tag{3.46}$$

Continuity of the total unsteady pressure (incident plus scattered) across the wake provides the boundary condition

$$e^{-iC_+}\left[\frac{\partial H_t}{\partial \Phi_t} - i\delta H_t\right]_{\Psi_t=0^+,\,\Phi_t>0} - e^{-iC_-}\left[\frac{\partial H_t}{\partial \Phi_t} - i\delta H_t\right]_{\Psi_t=0^-,\,\Phi_t>0} = -\frac{\Delta_p}{k^{3/2}} e^{iw\Phi_t}. \tag{3.47}$$

The formulation of the scattering problem is completed with the requirement of zero normal velocity on the airfoil, $\partial H_t/\partial \Psi_t = 0$ on $\Psi_t = 0$, $\Phi_t < 0$, as well as continuity of normal velocity across the wake:

$$e^{-iC_+}\left.\frac{\partial H_t}{\partial \Psi_t}\right|_{\Psi_t=0^+,\,\Phi_t>0} - e^{-iC_-}\left.\frac{\partial H_t}{\partial \Psi_t}\right|_{\Psi_t=0^-,\,\Phi_t>0} = 0. \tag{3.48}$$

The solution can be obtained with a straightforward application of the Wiener–Hopf technique. The result is

$$H_t = \frac{-\operatorname{sgn}(\Psi_t)\, i(2w)^{1/2}\Delta_p\, e^{iC_\pm}}{4\pi k^{3/2}} \int_{-\infty}^{\infty} \frac{\exp[-i\lambda\Phi_t - |\Psi_t|(\lambda^2 - w^2)^{1/2}]\, d\lambda}{(\lambda+\delta)(\lambda+w)(\lambda-w)^{1/2}}. \tag{3.49}$$

The plus sign in the constant $C_\pm$ applies for $\Psi_t > 0$ and the minus for $\Psi_t < 0$.

The asymptotic expansion of the local trailing-edge solution is required for matching with the trailing-edge ray field. Equation (3.49), when written in trailing-edge outer coordinates and expanded by the method of steepest descent, becomes

$$H_t = \frac{T(\theta_t)\, e^{ikwr_t}}{k^2 r_t^{1/2}} + O(k^{-3}, \alpha/k^2), \tag{3.50a}$$

where

$$T(\theta_t) = \frac{e^{-i\pi/4}\Delta_p \operatorname{sgn}(\psi_t)\, e^{iC_\pm}}{2[\pi w(1-\cos\theta_t)]^{1/2}(\delta - w\cos\theta_t)}. \tag{3.50b}$$

The directivity function $T(\theta_t)$ is singular for small values of θ_t, owing to the proximity

of the saddle point to the pole at $\lambda = -w$ in the integrand of (3.49) (see figure 3). The method of Van Der Waerden (1951) can be used to obtain an asymptotic expansion that is uniformly valid in θ_t:

$$H_t \sim \frac{-\Delta_p e^{iC_\pm}}{2k^{3/2}(\delta - w)}\left[i\,\mathrm{sgn}(\psi_t)\, e^{ikwr_t\cos\theta_t}\,\mathrm{erfc}\{e^{-i\pi/4}[kr_t\, w(1-\cos\theta_t)]^{1/2}\}\right.$$
$$\left. + \frac{e^{-i\pi/4}(2w)^{1/2}\sin\frac{1}{2}\theta_t\, e^{ikwr_t}}{(\pi kr_t)^{1/2}(\delta - w\cos\theta_t)}\right], \quad (3.51)$$

where erfc is the complementary error function (Abramowitz & Stegun 1972). For $O(1)$ values of θ_t, the asymptotic expansion of the complementary error function can be used to recover (3.50).

The local trailing-edge solution can now be matched with the outer solution to specify the undetermined amplitude of the trailing-edge rays. By replicating the leading-edge matching process which lead to (3.37), we find that

$$K_t(\theta_t) = T(\theta_t) \quad \text{and} \quad g_{1t}(\theta_t) = 0. \quad (3.52a, b)$$

Since the outer solution contains $T(\theta_t)$, it is also singular as θ_t approaches 0. The singularity signifies that the geometric-acoustics assumption of a slowly varying amplitude and rapidly varying phase is violated for small values of θ_t. An improved description of the sound field is needed in this 'transition' region, analogous to the zone in optical problems between illuminated and shadow regions. Our transition region is actually the union of two transition regions. For the wave on top of the airfoil, there exists an 'illuminated' region above the airfoil, a 'shadow' region below it, and a transition region between them. Similar regions exist for the wave below the airfoil, with the illuminated and shadow regions reversed. The transition region is shown in figure 2.

3.4. *Transition region*

The trailing-edge ray solution (3.39) becomes non-uniform when $\psi_t = O(k^{-1/2})$, as can be seen by comparing (3.50) and (3.51). In order to resolve this non-uniformity, a separate expansion is needed in the transition region where the rescaled variable

$$\eta = k^{1/2}\psi_t \quad (3.53)$$

is $O(1)$. We seek a solution which retains the phase dependence on the fast variable $k\phi_t$ and an amplitude dependence on the slow variable ϕ_t, but which also is a function of the transverse coordinate η whose scale is intermediate between the fast and slow variables. We attempt a solution of the form

$$h_{tn} = \frac{e^{ikw\phi_t}}{k^{3/2}}[h_{tn0}(\phi_t, \eta) + \alpha k^{1/2} h_{tn1}(\phi_t, \eta) + O(\alpha, 1/k, \alpha^2 k)]. \quad (3.54)$$

Like the local trailing-edge solution, the transition solution must cancel the jumps in pressure and vertical velocity across the wake due to the discontinuous leading-edge rays. However, in the transition region the $r^{-1/2}$ decay of the leading-edge field must be accounted for, as must non-uniform propagation effects.

To obtain the differential equation governing the transition field, we require the expansion of the mean-flow perturbation speed in transition coordinates:

$$q = \frac{1}{k^{1/2}}\frac{\eta}{\beta_\infty \phi_t^{1/2}(2+\phi_t)^{3/2}} + O(\alpha/k^{1/2}, 1/k^{3/2}). \quad (3.55)$$

Upon utilizing (3.53)–(3.55) in the homogeneous form of (2.4*b*), and imposing continuity of the total unsteady pressure and vertical velocity, we find at $O(k^{1/2})$ that

$$2\mathrm{i}w\frac{\partial h_{tn0}}{\partial \phi_t}+\frac{\partial^2 h_{tn0}}{\partial \eta^2}=0, \tag{3.56a}$$

$$\mathrm{e}^{-\mathrm{i}C_+}h_{tn0}|_{\eta=0^+}-\mathrm{e}^{-\mathrm{i}C_-}h_{tn0}|_{\eta=0^-}=\frac{\mathrm{i}\Delta_p}{w-\delta}\left(\frac{2}{2+\phi_t}\right)^{1/2}, \tag{3.56b}$$

$$\mathrm{e}^{-\mathrm{i}C_+}\frac{\partial h_{tn0}}{\partial \eta}\bigg|_{\eta=0^+}-\mathrm{e}^{-\mathrm{i}C_-}\frac{\partial h_{tn0}}{\partial \eta}\bigg|_{\eta=0^-}=0. \tag{3.56c}$$

The constants $\mathrm{e}^{-\mathrm{i}C_\pm}$ arise as a consequence of the transformation (2.4*a*) and the different values of ϕ resulting as a physical point on the wake sheet is approached from above or below.

The solution to the system of equations (3.56) may be found by employing a Laplace transform in the ϕ_t variable. With the aid of the convolution theorem, we find the result:

$$h_{tn0}=\frac{\operatorname{sgn}(\eta)\,\mathrm{i}\Delta_p\,\mathrm{e}^{\mathrm{i}C_\pm}}{(w-\delta)\sqrt{2}(2+\phi_t)^{1/2}}\mathrm{e}^{\mathrm{i}w\eta^2/2(2+\phi_t)}\operatorname{erfc}\left[\frac{\mathrm{e}^{-\mathrm{i}\pi/4}\,w^{1/2}|\eta|}{[\phi_t(2+\phi_t)]^{1/2}}\right]. \tag{3.57}$$

The function h_{tn0} describes the scattered field generated by the pressure discontinuity across the wake in the leading-edge ray field. The discontinuity in the vertical velocity of the leading-edge ray field generates the next term in the transition expansion.

The system of equations emerging at $O(\alpha k)$ is

$$2\mathrm{i}w\frac{\partial h_{tn1}}{\partial \phi_t}+\frac{\partial^2 h_{tn1}}{\partial \eta^2}=-\frac{2wV(0)\,\eta h_{tn0}}{\beta_\infty \phi_t^{1/2}(2+\phi_t)^{3/2}}, \tag{3.58a}$$

$$\mathrm{e}^{-\mathrm{i}C_+}h_{tn1}|_{\eta=0^+}-\mathrm{e}^{-\mathrm{i}C_-}h_{tn1}|_{\eta=0^-}=0, \tag{3.58b}$$

$$\mathrm{e}^{-\mathrm{i}C_+}\frac{\partial h_{tn1}}{\partial \eta}\bigg|_{\eta=0^+}-\mathrm{e}^{-\mathrm{i}C_-}\frac{\partial h_{tn1}}{\partial \eta}\bigg|_{\eta=0^-}=-\frac{V(0)\,\Delta_p\sqrt{2}\log(1+\phi_t+[\phi_t(2+\phi_t)]^{1/2})}{\beta_\infty(w-\delta)(2+\phi_t)^{3/2}}. \tag{3.58c}$$

A method similar to that used to solve the inhomogeneous equation (3.16) in the local leading-edge region can be utilized here. We attempt a solution containing combinations of inverse Laplace transforms:

$$h_{tn1}=\eta f_1(\phi)\int_{-\mathrm{i}\infty}^{\mathrm{i}\infty}C_1(s)\,\bar{h}(s,\eta)\,\mathrm{e}^{s\phi}\,\mathrm{d}s+f_2(\phi)\int_{-\mathrm{i}\infty}^{\mathrm{i}\infty}C_2(s)\,\bar{h}(s,\eta)\,\mathrm{e}^{s\phi}\,\mathrm{d}s. \tag{3.59}$$

The function $\bar{h}(s,\eta)$ is the Laplace transform of h_{tn0}, and f_1, f_2, C_1, and C_2 are to be determined. These functions are found by inserting (3.59) into the operator of (3.58*a*), differentiating under the integral signs and utilizing the differential equation (3.56*a*) for h_{tn0}, and then equating the result to the right-hand side of (3.58*a*) with h_{tn0} expressed as an inverse Laplace transform. The final result can be expressed in terms of the solution h_{tn0} and its derivatives:

$$h_{tn1}=\frac{\mathrm{i}}{\beta}V(0)\left(\frac{\phi_t}{2+\phi_t}\right)^{1/2}\eta h_{tn0}-\frac{V(0)}{\beta w}[[\phi_t(2+\phi_t)]^{1/2}-\log\{1+\phi_t+[\phi_t(2+\phi_t)]^{1/2}\}]\frac{\partial h_{tn0}}{\partial \eta}. \tag{3.60}$$

This particular solution satisfies the boundary conditions (3.58b, c); hence no complementary solution is required. The complete transition solution, with the terms in (3.60) written explicitly and combined, is

$$h_{tn} = \frac{\mathrm{i}\Delta_p \mathrm{e}^{\mathrm{i}C_\pm} \mathrm{e}^{\mathrm{i}kw\phi_t + \mathrm{i}w\eta^2/2\phi_t}}{k^{3/2}\sqrt{2(w-\delta)}(2+\phi_t)^{1/2}} \left\{ \mathrm{sgn}(\eta)\, \mathrm{e}^{-\mathrm{i}w\eta^2/\phi_t(2+\phi_t)} \,\mathrm{erfc}\left[\frac{\mathrm{e}^{-\mathrm{i}\pi/4} w^{1/2}|\eta|}{[\phi_t(2+\phi_t)]^{1/2}}\right] \right.$$
$$+ \frac{2\alpha k^{1/2}\mathrm{e}^{-\mathrm{i}\pi/4} V(0)}{(\pi w)^{1/2}\beta} + \frac{\alpha k^{1/2} V(0)}{\beta}\left[\frac{\mathrm{i}|\eta|}{2+\phi_t}\mathrm{e}^{-\mathrm{i}w\eta^2/\phi_t(2+\phi_t)}\,\mathrm{erfc}\left[\frac{\mathrm{e}^{-\mathrm{i}\pi/4} w^{1/2}|\eta|}{[\phi_t(2+\phi_t)]^{1/2}}\right]\right.$$
$$\left.\left. - \frac{2\mathrm{e}^{-\mathrm{i}\pi/4}}{[\pi w\phi_t(2+\phi_t)]^{1/2}}\right] \log\left(1+\phi_t+[\phi_t(2+\phi_t)]^{1/2}\right)\right\}. \quad (3.61)$$

It remains to establish that the transition solution h_{tn} asymptotically matches with the local trailing-edge solution and the outer trailing-edge ray solution. Matching with the local region does not alter the expressions already given for the transition solution, and hence is omitted, but we note that the argument closely follows that used by Myers & Kerschen (1992) to resolve undetermined eigenfunctions of the transition solution in a related problem. We concentrate instead on matching with the trailing-edge ray solution, which generates a common expansion used in composing a uniformly valid trailing-edge outer solution.

In the matching of the transition and trailing-edge outer solutions, the transition solution h_{tn} to $O(\alpha/k)$ is expressed in outer variables and expanded to $O(\alpha/k, 1/k^2)$, while the outer ray solution (3.39) to $O(1/k^2)$ is expressed in transition variables and expanded to $O(\alpha/k)$. The two expansions are identical and represent the common expansion. When expressed in transition variables the common expansion is

$$h_{com} = \frac{\mathrm{e}^{-\mathrm{i}\pi/4}\Delta_p \mathrm{e}^{\mathrm{i}C_\pm} \mathrm{e}^{\mathrm{i}kw\phi_t + \mathrm{i}w\eta^2/2\phi_t} \phi_t^{1/2}}{(2\pi w)^{1/2}(\delta - w)k^{3/2}\eta}\left[1 + \frac{\mathrm{i}\alpha k^{1/2}\eta V(0)}{\beta_\infty}\right.$$
$$\left. \times \left(\frac{\log\left(1+\phi_t+[\phi_t(2+\phi_t)]^{1/2}\right)}{\phi_t} - \frac{2}{[\phi_t(2+\phi_t)]^{1/2}}\right)\right]. \quad (3.62)$$

The uniformly valid trailing-edge outer solution $h_{t,u}$ is the trailing-edge ray field (3.39) plus the transition field (3.61) minus the common part:

$$h_{t,u} = h_t + h_{tn} - h_{com}. \quad (3.63)$$

The far-field form of $h_{t,u}$ is given in the next subsection.

3.5. *Total solution in the geometric far field*

At this point the solution to the convected-wave equation (2.4) has been determined in all of the asymptotic regions. We now collect the various terms into an expression for the total acoustic field in the geometric far field, $r \gg 1$. The far-field sound is expressed in leading-edge coordinates (r, θ). In the far field, the trailing-edge coordinates are related to the leading-edge coordinates by

$$r_t = r - [2 + \mathrm{sgn}(\psi)\,\alpha\pi/\beta_\infty]\cos\theta + O(1/r), \quad (3.64a)$$

$$\theta_t = \theta - [1 - \mathrm{sgn}(\psi)]\,\pi + O(1/r). \quad (3.64b)$$

The total solution is the sum of the outer leading-edge ray field (3.30) and the uniform outer trailing-edge solution (3.63). In the limit of $r \gg 1$, the total solution becomes

$$h_{total} \sim \frac{\exp[\mathrm{i}kwr + \mathrm{i}(\alpha k V(\theta)/\beta_\infty)\sin\theta \log 2r]}{k^{3/2} r^{1/2}}$$
$$\times \left\{ D(\theta) \exp[\mathrm{i}(\alpha k V(\theta)/\beta_\infty)[(\pi-\theta)\cos\theta + \sin\theta]] \right.$$
$$- \frac{\operatorname{sgn}(\psi)\,\Delta_p\, \mathrm{e}^{\mathrm{i}C_\pm}}{(2\pi)^{1/2}(\delta - w\cos\theta)} \exp[-2\mathrm{i}kw\cos\theta - \mathrm{i}(\alpha k/\beta_\infty)\pi w \operatorname{sgn}(\psi)\cos\theta]$$
$$\times \left[\pi^{1/2}\, \mathrm{i}\, \mathrm{e}^{-2\mathrm{i}kw(1-\cos\theta)} \operatorname{erfc}\{\mathrm{e}^{-\mathrm{i}\pi/4}[2kw(1-\cos\theta)]^{1/2}\} + \frac{\mathrm{e}^{-\mathrm{i}\pi/4}}{[2kw(1-\cos\theta)]^{1/2}} \right.$$
$$\left. \left. - \frac{\mathrm{e}^{-\mathrm{i}\pi/4} \exp[-\mathrm{i}(\alpha k V(\theta)/\beta_\infty)[(\theta - \pi + \pi \operatorname{sgn}(\psi))\cos\theta + \sin\theta]]}{[2kw(1-\cos\theta)]^{1/2}} \right] \right\}. \tag{3.65}$$

The leading-edge directivity series $D(\theta)$ is given in (3.37*a*), (3.8*b*), (3.11*b*), (3.15*b*, *d*), and (3.26c). The function $V(\theta)$ is defined in (3.35*b*) and the constants Δ_p and $\mathrm{e}^{\mathrm{i}C_\pm}$ in (3.45). The terms proportional to the pressure jump Δ_p represent the far-field expansion of the uniform trailing-edge solution defined in (3.63).

The far-field form of the modified pressure, derived from (2.8), is

$$p_{total} = -\mathrm{i}k(\delta - w\cos\theta)\, \mathrm{e}^{-\mathrm{i}k\delta M_\infty^2 r\cos\theta} h_{total}. \tag{3.66}$$

4. Results and discussion

4.1. *Summary of solution structure*

The solution structure in each of the asymptotic regions reveals much about the physics of sound generated by the interaction of high-frequency convected disturbances with aerodynamically loaded airfoils. Below we summarize the results of §3, noting the reduced form of the wave operator and the type of solution in each region.

In the local leading-edge region, the only relevant lengthscale is the disturbance wavelength. The complete differential equation and boundary conditions may be approximated by uniform-medium components plus a perturbation series beginning at order $\alpha k^{1/2}$, this quantity being considered a small parameter. Physically, $\alpha k^{1/2}$ is proportional to the square root of the shift of the mean-flow stagnation point from the leading edge, scaled on the gust wavelength. The solution contains a term H_0 corresponding to a uniform mean flow, plus three additional $O(\alpha k^{1/2})$ terms, H_1, H_2, and H_3, due to mean-loading effects. The term H_1 arises from the change in the boundary condition on the airfoil surface, due to distortion of the vortical gust by mean-flow gradients. H_2 is due to the volume sources arising from variations in the Reynolds-stress components involving products of the unsteady vortical velocity and the mean-flow gradients. Distortion of the entropy disturbance by mean-flow gradients also contributes to the source term for H_2. As discussed below, the volume source can be related to quadrupole sources contained in the acoustic analogy. The function H_3 is generated by the interaction between the field H_0 and the local variations in mean-flow velocity and speed of sound contained in the perturbation operator L_1. Since these local variations have the same lengthscale as the acoustic wave, this interaction results in additional sound radiation.

In the outer region two lengthscales are relevant: the airfoil chord, which characterizes changes in the propagation medium, and the disturbance wavelength. Both of the operators L_0 and L_1 of the wave equation (2.4*b*) must be considered in the leading approximation. However, the analysis is simplified by the multiple-scales

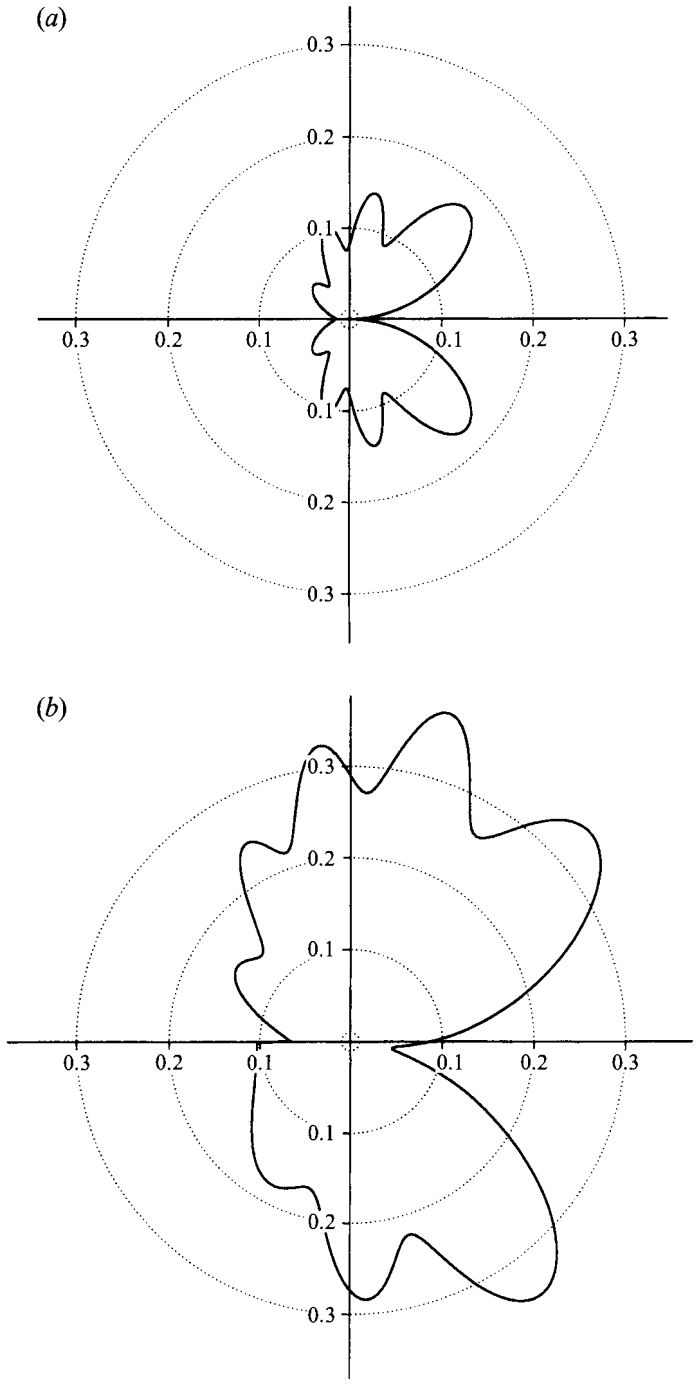

FIGURE 4(*a*, *b*). For caption see facing page.

behaviour. A volume source is also present in the outer region, but it gives rise to a multiple-scales solution with a convected phase. The convection of this disturbance by the slowly varying mean flow does not contribute to the acoustic field, which is a geometric–acoustic solution to the homogeneous wave equation. The mean-flow variation produces $O(1)$ phase shifts which are captured naturally as distortions to the

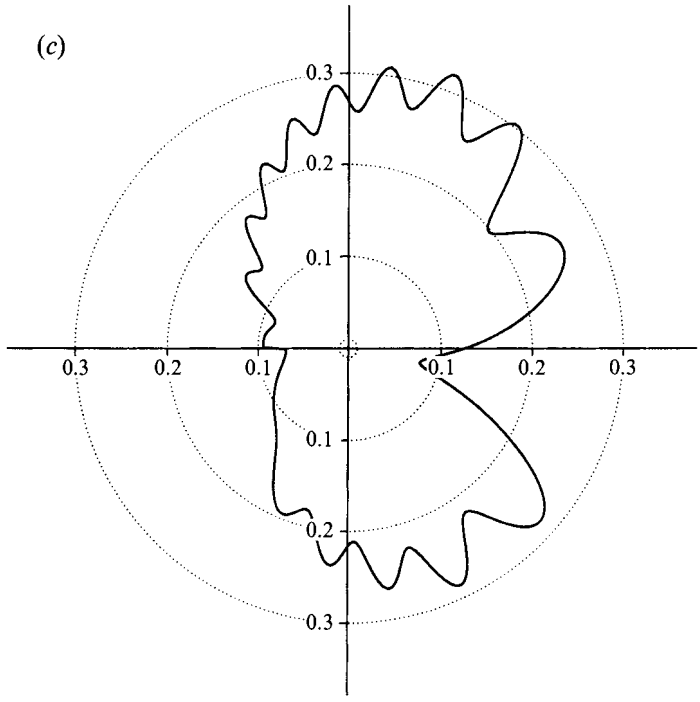

FIGURE 4. Far-field pressure directivity pattern for $M_\infty = 0.6$: (*a*) $\alpha = 0$, $k = 6$, $\theta_g = 45°$; (*b*) $\alpha = 6°$, $k = 6$, $\theta_g = 45°$; (*c*) $\alpha = 6°$, $k = 12$, $\theta_g = 45°$.

cylindrical-wave phase appropriate for a uniform medium. The initial conditions for the acoustic rays in the outer region are provided by the asymptotic expansions of the local leading-edge and local trailing-edge solutions.

In the local trailing-edge region, the mean flow is nearly uniform owing to the imposition of the Kutta condition. Thus, the sound sources in the local trailing-edge region due to mean-flow gradients (corresponding to the terms H_1, H_2, and H_3 in the local leading-edge region) are of higher order and can be neglected. The trailing edge generates sound only by scattering leading-edge rays, which have undergone different $O(1)$ phase shifts in propagating along the two surfaces of the airfoil. This local field scattered by the trailing edge is a solution to the uniform-medium Helmholtz equation. The saddle-point asymptotic expansion of the local trailing-edge solution, and consequently the amplitude of the trailing-edge ray field, are singular at shallow angles to the downstream direction. The singularity is evidence of the need for a description different than geometric acoustics in a narrow 'transition' region behind the airfoil.

The extent of the transition boundary layer is θ_t (or ψ_t) $= O(k^{-1/2})$. A parabolic differential equation approximates the full wave equation in the transition region, and jump conditions across the wake are required to cancel discontinuities in the leading-edge ray field. The solution maintains a rapidly varying phase, but the amplitude acquires a dependence on the intermediate variable $k^{1/2}\theta$ (or $k^{1/2}\psi$). At larger angles (where the asymptotic expansion of the error-function solution is appropriate) the amplitude develops the slowly varying behaviour necessary for matching with geometric acoustics.

With increases in α and/or k, the far-field sound becomes strongly influenced by the $O(\alpha k^{1/2})$ sources in the local leading-edge region. Because the trailing-edge ray field is weaker than the leading-edge ray field by $O(k^{-1/2})$, and because the extent of the

transition region is $O(k^{-1/2})$, the influence of trailing-edge scattering becomes weaker as k is increased. These trends are illustrated by numerical results presented in the next section.

4.2. *Numerical results*

We postpone a thorough parametric study of the solution until a subsequent publication (Myers & Kerschen 1995), where generalizations will have been made to include the effects of airfoil camber. Here we demonstrate the importance of incidence angle for a selected set of mean-flow and disturbance parameter values. The characteristics of the acoustic field are illustrated through pressure directivity patterns and computations of total acoustic power.

The pressure directivity patterns are plotted as a function of angle at a constant distance from the leading edge in the physical plane. The far-field relations between the Prandtl–Glauert, potential-streamline coordinates (r, θ) used throughout the analysis and the physical coordinates (r_{ph}, θ_{ph}) are

$$\tan\theta = \beta_\infty \tan\theta_{ph}, \tag{4.1}$$

$$r = (1 - M_\infty^2 \sin^2\theta_{ph})^{1/2} r_{ph}, \tag{4.2}$$

where r_{ph} is distance from the leading edge, normalized by the airfoil semi-chord b. The pressure directivity which we plot is the far-field value of $|p|_{ph}^{r^{1/2}}$, where the modified pressure p is defined by (2.8) and (3.66).

A set of pressure directivity patterns is presented for the case where the free-stream Mach number is 0.6 and the high-frequency parameter k is 6. The gust is assumed to be two-dimensional ($A_3 = k_3 = 0$) and purely vortical (entropy amplitude $B = 0$), with an orientation angle θ_g (the angle between the gust wavevector and mean velocity far upstream) of 45°. Since the magnitude of the vortical velocity is contained in the small parameter ϵ, we take $|A| = 1$. Then, from (2.3d), we find that $A_n = -0.707$, $A_t = 0.707$, and $k_n = 1.25$. Figure 4(a) contains the directivity pattern for zero incidence angle. In this case the leading-edge rays travelling just above and below the airfoil are 180° out of phase at the trailing edge, and hence on the wake the entire leading-edge ray field is cancelled by the transition field. The lobes generated by the interference between the leading-edge and trailing-edge rays are also visible on the plot.

The parameters for figure 4(b) are the same as those for 4(a), except the incidence angle has been raised to 6°. Even for this small incidence angle, the overall level of the acoustic pressure has increased by a factor of approximately two. The sound pressure above the airfoil is somewhat larger than that below. A slight amount of radiation directly downstream can be seen, as can a jump in pressure directly in front of the airfoil. This jump is due to a discontinuity in the trailing-edge rays across the leading edge, and would be corrected at the next order in the analysis by a leading-edge scattered field. Note that the minimum pressure in figure 4(b) occurs at a shallow angle below the wake, rather than directly behind the airfoil.

For the final directivity pattern in figure 4(c), the incidence angle is again 6° but the dimensionless frequency k has been raised from 6 to 12. The overall level of the sound pressure in figure 4(c) is quite close to that for figure 4(b). For comparison, the zero-incidence-angle result for $k = 12$ is obtained by multiplying the values in figure 4(a) by $1/\sqrt{2}$. Thus, at this higher frequency, the introduction of a 6° incidence angle has caused a proportionately larger increase in the acoustic pressure level, consistent with the $O(\alpha k^{1/2})$ amplitude scaling for the incidence angle effects. The sound radiation above the airfoil in figure 4(c) is somewhat stronger than that below, as was the case in figure 4(b). Also, there is again a slight discontinuity in pressure in front of the airfoil. In the $k = 12$ case, however, there is much more radiation directly behind the

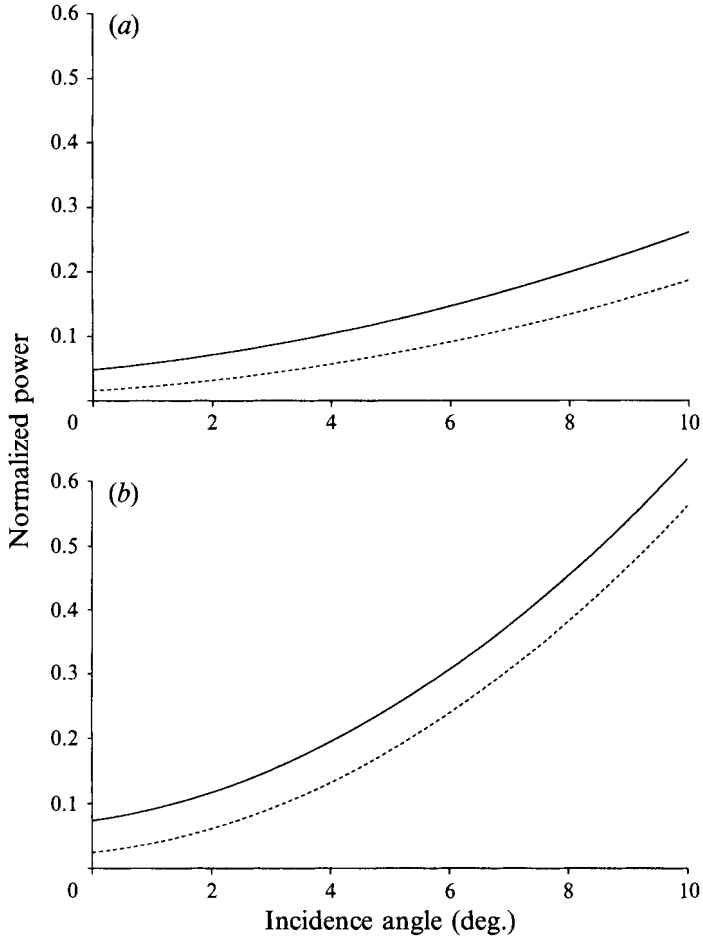

FIGURE 5. Radiated acoustic power *vs.* incidence angle. $k = 7$, $\theta_g = 30°$ (solid line) and 60° (dashed line). (*a*) $M_\infty = 0.5$, (*b*) $M_\infty = 0.75$.

airfoil. As expected at the higher frequency, the modulation of the directivity pattern due to leading-edge/trailing-edge interference is more rapid, and the interference lobes are smaller because of the decreased intensity of the trailing-edge field relative to that of the leading edge. There are approximately twice as many interference lobes above the airfoil than below it, illustrating another manner in which the small incidence angle has destroyed the symmetric pattern which occurs in the case of an unloaded flat-plate airfoil.

To calculate acoustic power, we use the definition of acoustic intensity

$$I = \left[\frac{p'}{\rho_0} + \nabla G' \cdot \boldsymbol{U}_0\right](\rho_0 \nabla G' + \rho' \boldsymbol{U}_0). \tag{4.3}$$

Blokhintsev (1956) showed that this acoustic energy flux is a conserved quantity in the geometric acoustics limit (sound wavelength short compared to the scale on which the mean flow varies), which applies in the outer region of the present problem. It should be noted that the acoustic intensity is not a measure of the total energy flux of the unsteady motion, which also has contributions from the vortical and entropic disturbances. General discussions of energy relations in non-uniform flows can be found in Morfey (1971) and Myers (1991), and in the references cited therein. Our

interest is only in the acoustic power generated by the airfoil–gust interaction, and this can be found by integrating the acoustic intensity over a closed surface in the far field. We proceed by transforming to the reduced potential h (via (2.4a) and (2.7)), integrating over a large circle ($r \gg 1$) in (ϕ, ψ)-space (an ellipse in physical space), and taking the time average. After non-dimensionalization, the expression for time-averaged power-per-unit-span becomes

$$\text{Normalized power} = \frac{\text{Average power/span}}{\frac{1}{2}\rho_\infty U_\infty^3 b\epsilon^2}$$

$$= k^2 w \int_0^{2\pi} hh^*(\beta_\infty \cos^2\theta + \sin^2\theta)(\beta_\infty^2 \sin^2\theta + \cos^2\theta)^{1/2} r \, \mathrm{d}\theta, \quad (4.4)$$

where b is the airfoil semi-chord, ϵ the normalized gust velocity (see (2.3)), the far-field potential h is given by (3.65) and h^* is the complex conjugate of h.

The amount of radiated sound power is plotted as a function of incidence angle in figure 5(a). Here $M_\infty = 0.5$, $k = 7$, and $\theta_g = 30°$ and 60°. A marked increase in power occurs with increasing incidence angle for both gust orientations; when the incidence angle has reached just 10° the normalized power has risen by a factor of about 5. The increase is even sharper at the higher Mach number of 0.75, as shown in figure 5(b). A ten-fold rise in power can be seen with an increase in incidence angle of only 10°, for both gust orientations. On the basis of the small parameter space examined here, we conclude that the radiated sound field for high-frequency gust interactions is quite sensitive to the incidence angle of the airfoil.

4.3. *Comparison with acoustic analogy theories*

Much of the present understanding of sound generated by gust–airfoil interactions has been gained through the use of Lighthill's acoustic analogy. The operator utilized in acoustic-analogy approaches corresponds to linear propagation in a uniform medium, either at rest or in uniform motion. The effects of variations in the mean-flow properties appear in the quadrupole-source term, which is expressed in terms of flow variables whose values are not known *a priori* but would be determined in the course of solving the original nonlinear equations. Thus, effective use of the acoustic analogy requires that the dominant components of the quadrupole source be identified, and that heuristic models for these source terms be introduced.

In their treatment of fan noise via the acoustic analogy, Ffowcs-Williams & Hawkings (1969b) neglected the 'non-uniform acoustic medium' effects and modelled the portion of the Reynolds stress representing the interaction of the steady potential flow with the vortical velocity. They concluded that the noise intensity produced by the free (volume) quadrupoles depends upon the eighth power of the mean-flow Mach number. For comparison, the usual compact-surface radiation first obtained by Curle (1955) scales as M^6. Thus, Ffowcs Williams & Hawkings concluded that, at high subsonic Mach numbers, the free quadrupole sources might become important relative to the radiation from dipole sources on the airfoil surface. Ffowcs Williams & Hall (1970) subsequently developed the concept of scattered quadrupole sources, which are present when a free quadrupole radiates in the presence of an extended surface with a sharp edge. They showed that the scattered quadrupole source radiates with an efficiency of M^5, and hence at low Mach numbers dominates both the free-quadrupole radiation and the dipole radiation from a compact surface. The Mach-number dependencies quoted thus far apply to three-dimensional sources. For two-dimensional problems (e.g. a two-dimensional convected gust interacting with an infinite-span

airfoil) the efficiencies have the power of M reduced by one. The compact-surface dipole radiation thus scales as M^5, the free quadrupole as M^7, and the scattered quadrupoles as M^4.

The rapid-distortion approach to sound prediction utilized in this study differs from approaches based upon the acoustic analogy in several respects. For the rapid-distortion approach, the differential operator in (2.1*b*) governing the unsteady motion corresponds to the linear convected-wave equation for a medium with variable mean velocity U_0, density ρ_0 and speed of sound a_0. The source term in (2.1*b*) is given explicitly in terms of the convected disturbance far upstream and mean flow-field quantities. In contrast to the acoustic analogy, the rapid-distortion approach avoids the need for source modelling. Of course, it must be remembered that the acoustic analogy is a general formulation that is applicable to a wide variety of noise-generation mechanisms. Goldstein's (1978) rapid-distortion theory is applicable only to noise generated by the interaction of unsteady convected disturbances with steady potential flows.

Owing to the very different formulations of the two theories, a general comparison between the rapid-distortion and acoustic-analogy approaches to the present problem is difficult. However, if attention is restricted to the airfoil leading-edge region and to low Mach numbers, a meaningful comparison can be made. At low Mach numbers, the acoustic wavelength is large and the trailing-edge field can be comparable to the leading-edge field (unless the airfoil is long compared to the acoustic wavelength). However, since the trailing edge just scatters the sound generated at the leading edge, a focus on the leading-edge region remains physically meaningful for the case of short-wavelength gusts in the low-Mach-number limit.

To compare rapid-distortion theory with the acoustic analogy, we revert to the physical variables introduced in §2. In the local leading-edge region, the mean flow and substantial derivative have the expansions

$$\boldsymbol{U}_0(\boldsymbol{x}) = \boldsymbol{U}_\infty + \alpha k^{1/2}\boldsymbol{u}^p(\boldsymbol{x}) \tag{4.5a}$$

and

$$\frac{\mathrm{D}_0}{\mathrm{D}t} = \frac{\partial}{\partial t} + \boldsymbol{U}_\infty\cdot\boldsymbol{\nabla} + \alpha k^{1/2}\boldsymbol{u}^p\cdot\boldsymbol{\nabla} = \frac{\mathrm{D}_\infty}{\mathrm{D}t} + \alpha k^{1/2}\boldsymbol{u}^p\cdot\boldsymbol{\nabla}. \tag{4.5b}$$

The unsteady quantities consist of an $O(\epsilon)$ term present for a uniform mean flow, plus an $O(\epsilon\alpha k^{1/2})$ correction which accounts for the influence of a variable mean flow. The vortical velocity, unsteady potential, and unsteady pressure have expansions of the form

$$\boldsymbol{v}' = \epsilon\boldsymbol{v}_0' + \epsilon\alpha k^{1/2}\boldsymbol{v}_1', \tag{4.6a}$$

$$G' = \epsilon G_0' + \epsilon\alpha k^{1/2} G_1', \tag{4.6b}$$

and

$$p' = \epsilon p_0' + \epsilon\alpha k^{1/2} p_1'. \tag{4.6c}$$

If we utilize the substantial derivative (4.5*b*) and the potential function (4.6*b*) in (2.1*c*), and ignore $O(M_\infty^2)$ terms ($a_0 = a_\infty[1+O(M_\infty^2)]$, $\rho_0 = \rho_\infty[1+O(M_\infty^2)]$), we find that the first-order correction to the unsteady pressure is given by

$$p_1' = -\rho_\infty \frac{\mathrm{D}_\infty G_1'}{\mathrm{D}t} - \rho_\infty \boldsymbol{u}^p\cdot\boldsymbol{\nabla} G_0'. \tag{4.7}$$

The governing equation for p_1' is obtained by applying (4.5*b*) to the wave equation (2.1*b*), with G' prescribed by (4.6*b*). After using the fact that $\boldsymbol{u}^p$ is solenoidal at low Mach numbers, and again ignoring $O(M_\infty^2)$ terms, we obtain

$$\frac{1}{a_\infty^2}\frac{\mathrm{D}_\infty^2 p_1'}{\mathrm{D}t^2} - \nabla^2 p_1' = -\rho_\infty \frac{\partial}{\partial x_i}\frac{\mathrm{D}_\infty v_{1i}'}{\mathrm{D}t} + 2\rho_\infty \frac{\partial}{\partial x_i}\frac{\partial}{\partial x_j}\left(u_i^p \frac{\partial G_0'}{\partial x_j}\right). \tag{4.8}$$

(The term $(1/a_\infty^2)\mathrm{D}_\infty^2 p_1'/\mathrm{D}t^2$ is $O(M_\infty^2)$ and could be neglected, but is retained for subsequent comparisons.) The source term containing the derivative of v_{1i}' can be simplified using the governing equation for the vortical velocity (Goldstein 1978):

$$\frac{\mathrm{D}_0 \boldsymbol{v}'}{\mathrm{D}t} + \boldsymbol{v}' \cdot \boldsymbol{\nabla} \boldsymbol{U}_0 = 0. \tag{4.9}$$

Upon inserting (4.5*a*, *b*) and (4.6*a*) in (4.9) and extracting the $O(\epsilon\alpha k^{1/2})$ component, introducing the result in (4.8), and utilizing the fact that both $\boldsymbol{v}_0'$ and $\boldsymbol{u}^p$ are solenoidal, we arrive at the final form of the governing equation for p_1':

$$\frac{1}{a_\infty^2}\frac{\mathrm{D}_\infty^2 p_1'}{\mathrm{D}t^2} - \nabla^2 p_1' = 2\rho_\infty \frac{\partial}{\partial x_i}\frac{\partial}{\partial x_j}(u_i^p u_{0j}'), \tag{4.10}$$

where $\boldsymbol{u}_0' = \boldsymbol{v}_0' + \boldsymbol{\nabla} G_0'$ is the total $O(\epsilon)$ unsteady velocity.

The boundary condition for p_1' is derived by applying (4.5*b*) to (2.1*d*), with the vortical velocity and potential function given by (4.6*a*) and (4.6*b*). The resulting equation is

$$n_i \frac{\partial p_1'}{\partial x_i} = -\rho_\infty n_i \left(\frac{\partial u_j^p}{\partial x_i}\frac{\partial G_0'}{\partial x_j} + v_{0j}'\frac{\partial u_i^p}{\partial x_j} \right). \tag{4.11}$$

After expanding the implied summation, inserting the specific form $\boldsymbol{u}^p = (2/R)^{1/2} \times (\cos\frac{1}{2}\theta, \sin\frac{1}{2}\theta)$, and using (2.1*d*) to equate v_{02}' with $-\partial G_0'/\partial x_2$, we find that the right-hand side of (4.11) vanishes; hence, the boundary condition on the airfoil surface is simply

$$n_i \, \partial p_1'/\partial x_i = 0. \tag{4.12}$$

We next examine the present problem from the viewpoint of the acoustic analogy. Consider the well-recognized form of Lighthill's equation (Ffowcs Williams & Hall 1970)

$$\frac{1}{a_\infty^2}\frac{\partial^2 p'}{\partial t^2} - \nabla^2 p' = \frac{\partial}{\partial x_i}\frac{\partial}{\partial x_j}(\rho u_i u_j), \tag{4.13}$$

where u_i represents the total velocity and ρ the total density. In the local leading-edge region we decompose the total velocity into the sum of a uniform mean flow $\boldsymbol{U}_\infty$, an $O(\alpha k^{1/2})$ steady perturbation velocity $\boldsymbol{u}^p$, and an $O(\epsilon)$ unsteady velocity $\boldsymbol{u}'$. The total density has a similar decomposition, except that the steady-flow perturbation density is $O(M_\infty^2)$ relative to the uniform density and is ignored. If we incorporate these velocity and density decompositions in (4.13), convert to a convected-wave equation (with the aid of the continuity equation), and retain the lowest-order ($O(\epsilon\alpha k^{1/2})$) time-dependent source term, we arrive at an equation describing the effects of mean-flow variations on the sound field:

$$\frac{1}{a_\infty^2}\left[\frac{\partial}{\partial t} + \boldsymbol{U}_\infty \cdot \boldsymbol{\nabla}\right]^2 p' - \nabla^2 p' = 2\rho_\infty \frac{\partial}{\partial x_i}\frac{\partial}{\partial x_j}(u_i^p u_{0j}'). \tag{4.14}$$

Equation (4.14) is identical to equation (4.10) governing the $O(\epsilon\alpha k^{1/2})$ pressure p_1' in rapid-distortion theory. When the usual boundary condition $\partial p'/\partial n = 0$ is imposed on the solution of (4.14), the boundary conditions for the acoustic analogy and rapid distortion theory are identical as well.

The above analysis shows that, at low Mach numbers, the equations governing the $O(\epsilon\alpha k^{1/2})$ components of the pressure fields in the acoustic analogy and rapid-distortion theory formulations are consistent in the local leading-edge region. The

practical application of the two theories, however, manifests differences. Proper utilization of the acoustic analogy requires knowledge of the total $O(\epsilon)$ unsteady velocity, which includes the lowest-order irrotational velocity $\nabla G_0'$. Since $\nabla G_0'$ is not known in a simple form, quantitative modelling of the source term (e.g. for use in a Green's function integral) can become difficult. The rapid-distortion approach, while written as a quadrupole source for comparison purposes above, is developed systematically in §3 as a sequence of boundary-value problems. No modelling of source terms is required.

The similarity between the volume source giving rise to the local leading-edge solution H_2 and the quadrupole source of the acoustic analogy was noted in §3.1.3. However, H_2 is not the same as the solution to (4.10)–(4.12), even after converting the dependent variable from potential to pressure. The reason is that vorticity distortion on the airfoil surface, represented by the last term in boundary condition (4.11), is split off from the problem formulation for H_2 and contained in the boundary condition for H_1. This split, which is logical from the point of view of physical effects, has the unorthodox consequence of creating cancelling monopoles in the solutions for H_1 and H_2 at low Mach numbers. Each monopole field radiates with an intensity proportional to M^3. When the solutions H_1 and H_2 are combined, we recover the appropriate M^4 behaviour derived by Ffowcs Williams & Hall (adjusted for two dimensions) for a scattered quadrupole. In discussing volume-source solutions, then, H_2 should be considered in conjunction with H_1 when the Mach number is small.

A final remark relating the present theory to the acoustic analogy at low Mach numbers concerns our solution H_0, which does not involve mean-loading effects. This term arises solely from the unsteady pressure on the airfoil surface, and can be thought of as a distribution of dipoles similar to the point dipoles originally modelled by Curle. However, the intensity associated with H_0 scales as M^4, corresponding to a pole of 3/2 order, rather than as M^5 for the case of an isolated two-dimensional dipole. The increase in efficiency over that for an isolated dipole has come about due to non-compactness effects. The result of Ffowcs Williams & Hall has sometimes been interpreted to imply that 'scattered quadrupole' sources dominate over 'surface dipole' sources at low Mach numbers. The present results show that, at low Mach numbers, the non-compact surface sources and the scattered quadrupole sources are of equal importance. In fact, H_0 and the combination $H_1 + H_2$ also have the same $\cos\frac{1}{2}\theta$ pressure directivity pattern, in addition to the same scaling on Mach number.

For high subsonic Mach numbers, one might anticipate that the influence of non-uniform-propagation effects could be quite important. An advantage of the theory presented in this paper over theories based on the acoustic analogy is the natural inclusion of variations in the properties of the medium. As noted earlier, these variations generate additional sound in the local leading-edge region through the solution H_3. For $O(1)$ Mach numbers, the source region is non-compact and source classifications with respect to pole order are not useful. Rather, the important feature for high subsonic Mach numbers is the scaling with respect to the Prandtl–Glauert factor, $\beta_\infty = (1 - M_\infty^2)^{1/2}$. For small β_∞, the acoustic intensities associated with H_0, H_1, H_2, and H_3 are proportional to β_∞^{-2}, β_∞^{-4}, β_∞^{-6}, and β_∞^{-8}, respectively. Strictly speaking, our theory is not valid in the limit $M \to 1$ because our expressions for the mean-flow perturbation become singular. Nevertheless, our solution suggests that local scattering by the non-uniform medium is an important sound-generation mechanism at high subsonic Mach numbers. We defer a full numerical study of the Mach-number dependence of the different sound sources to the forthcoming paper (Myers & Kerschen 1995), which incorporates airfoil camber into the theory.

Much of the work described herein was funded by NASA Lewis Research Center under grant NAG3-357. We gratefully acknowledge this support. We thank Professor T. F. Balsa and other colleagues at the University of Arizona for many stimulating and productive discussions. Dr Chung-Tien Tsai contributed to the analysis of the transition region and the eigenfunctions of H_3. We also express our gratitude for computer support from the Division of Electronics and Computer Science of the FDA, especially the assistance of Bruce Danielson.

Appendix

In this Appendix we calculate the complementary solution H_{2c} to the local leading-edge particular solution H_{2p}.

The normal velocity on the airfoil surface associated with H_{2p} is

$$\left.\frac{\partial H_{2p}}{\partial \Psi}\right|_{\Psi=0} = \frac{1}{(2\pi)^{1/2}} \int_{-\infty}^{\infty} B(\lambda)\, \mathrm{e}^{-\mathrm{i}\lambda\Phi}\, \mathrm{d}\lambda, \tag{A 1}$$

where

$$B(\lambda) = \frac{\mathrm{e}^{\mathrm{i}\pi/4}}{4\sqrt{2}(\delta^2+k_n^2)} \left[(\lambda+\delta')^{1/2} f_2(\lambda) + \frac{\mathrm{i}k_n f_1(\lambda)}{(\lambda+\delta')^{1/2}} - \frac{(\lambda^2-w^2)^{1/2} f_2(\lambda)}{(\lambda+\delta)^{1/2}} \right] \frac{1}{(\lambda-\lambda_1)(\lambda-\lambda_2)}. \tag{A 2}$$

The quantities λ_1, λ_2, f_1, and f_2 are defined in (3.13). To cancel (A 1), a complementary solution H_{2c} satisfying

$$\mathrm{L}(H_{2c}) = 0, \tag{A 3a}$$

$$\left.\frac{\partial H_{2c}}{\partial \Psi}\right|_{\Psi=0} = -\frac{1}{(2\pi)^{1/2}} \int_{-\infty}^{\infty} B(\lambda)\, \mathrm{e}^{-\mathrm{i}\lambda\Phi}\, \mathrm{d}\lambda \quad \text{for} \quad \Phi > 0, \tag{A 3b}$$

$$H_{2c}|_{\Psi=0^-}^{\Psi=0^+} = 0 \quad \text{for} \quad \Phi < 0, \tag{A 3c}$$

and

$$\partial H_{2c}/\partial \Psi \quad \text{continuous everywhere} \tag{A 3d}$$

is required. The operator L in (A 3a) is the Helmholtz operator defined in (3.5c).

We apply a Fourier transform in Φ to (A 3) and solve the resulting ordinary differential equation. The result can be written as

$$H_{2c} = \mathrm{sgn}(\Psi) \int_{-\infty}^{\infty} C_+(\lambda) \exp\left[-\mathrm{i}\lambda\Phi - |\Psi|(\lambda^2-w^2)^{1/2}\right] \mathrm{d}\lambda. \tag{A 4}$$

The plus subscript on the unknown function $C(\lambda)$ indicates that it is analytic in the upper half-plane, which is necessary in order that the potential be continuous across $\Psi = 0$ in front of the airfoil, thereby satisfying (A 3c). To determine $C_+(\lambda)$ we proceed by introducing the unknown function $u(\Phi)$ defined by

$$\left.\frac{\partial H_{2c}}{\partial \Psi}\right|_{\Psi=0} = u(\Phi) - \frac{1}{(2\pi)^{1/2}} \int_{-\infty}^{\infty} B(\lambda)\, \mathrm{e}^{-\mathrm{i}\lambda\Phi}\, \mathrm{d}\lambda. \tag{A 5}$$

By the boundary condition (A 3b), $u(\Phi) = 0$ for $\Phi > 0$. Upon Fourier transforming (A 5) and dividing the result by $(\lambda-w)^{1/2}$, we obtain

$$-(\lambda+w)^{1/2} C_+(\lambda) = \frac{U_-(\lambda)}{(\lambda-w)^{1/2}} - \frac{B(\lambda)}{(\lambda-w)^{1/2}}. \tag{A 6}$$

The minus subscript on $U_-(\lambda)$ denotes analyticity in the lower half-plane.

The last term in (A 6) is next split into the sum of two functions, each analytic in one half-plane. By observing the location of the various poles and branch points in figure 3, we see that $B(\lambda)/(\lambda-w)^{1/2}$ may be written as

$$\frac{B(\lambda)}{(\lambda-w)^{1/2}} = \frac{D_-(\lambda)+D_+(\lambda)}{(\lambda-\lambda_1)(\lambda-\lambda_2)}, \tag{A 7a}$$

where

$$D_-(\lambda) = \frac{\mathrm{e}^{\mathrm{i}\pi/4}}{4\sqrt{2}(\delta^2+k_n^2)}\left[\frac{(\lambda+\delta')^{1/2}f_2(\lambda)}{(\lambda-w)^{1/2}}+\frac{\mathrm{i}k_n f_1(\lambda)}{(\lambda-w)^{1/2}(\lambda+\delta')^{1/2}}\right] \tag{A 7b}$$

and

$$D_+(\lambda) = \frac{-\mathrm{e}^{\mathrm{i}\pi/4}}{4\sqrt{2}(\delta^2+k_n^2)}\frac{(\lambda+w)^{1/2}f_2(\lambda)}{(\lambda+\delta)^{1/2}}. \tag{A 7c}$$

Once again the plus and minus subscripts denote the region of analyticity. It is fortunate that $B(\lambda)/(\lambda-w)^{1/2}$ can be written as the sum of terms each having branch points all in the same half-plane. The resulting Wiener–Hopf split only involves separating terms with simple-pole singularities. After completing the split of (A 7*a*), inserting the result into (A 6), and rearranging terms, we have

$$\begin{aligned}-(\lambda+w)^{1/2}C_+(\lambda)+\frac{D_-(\lambda_2)}{(\lambda_2-\lambda_1)(\lambda-\lambda_2)}+\frac{D_+(\lambda)}{(\lambda-\lambda_1)(\lambda-\lambda_2)}-\frac{D_+(\lambda_1)}{(\lambda-\lambda_1)(\lambda_1-\lambda_2)}\\ =\frac{U_-(\lambda)}{(\lambda-w)^{1/2}}-\frac{D_-(\lambda)}{(\lambda-\lambda_1)(\lambda-\lambda_2)}+\frac{D_-(\lambda_2)}{(\lambda_2-\lambda_1)(\lambda-\lambda_2)}-\frac{D_+(\lambda_1)}{(\lambda-\lambda_1)(\lambda_1-\lambda_2)}.\end{aligned} \tag{A 8}$$

The left-hand side of (A 8) is analytic in the upper half-plane, the right-hand side is analytic in the lower half-plane, and the two sides are equal on the strip $\mathrm{Im}(-w) < \mathrm{Im}(\lambda) < \mathrm{Im}(w)$. They are thus analytic continuations of one another and form an entire function. We turn to the edge conditions in the physical plane to determine the unknown analytic function.

The edge condition we impose is that the solution H_{2c} be no more singular near the origin than the zero-incidence angle solution H_0. The solution H_0 possesses a $R^{1/2}$ singularity ($R^2 = \Phi^2+\Psi^2$) as R approached zero. This same edge behaviour arises naturally in the particular solution H_{2p} obtained by double Fourier transforms. Thus we require that H_{2c} behave as $R^{1/2}$ locally, and hence that the transform function $C_+(\lambda)$ decay as $\lambda^{-3/2}$ in the upper half-plane (Noble 1958).

The entire function defined by (A 8) can be determined by analysing the left-hand side as λ tends to infinity in the upper half-plane. The first, second, and fourth terms decay to zero and the third approaches a limiting value of

$$-4\mathrm{i}k_nC_4-4\mathrm{i}\delta C_3. \tag{A 9}$$

Hence the bounded, entire function is equal to the constant in (A 9). Setting the left-hand side of (A 8) equal to this constant, inserting the resulting expression for $C_+(\lambda)$ back into (A 4), and writing D_- and D_+ explicitly yields the final form of the solution:

$$\begin{aligned}H_{2c} = -\frac{\mathrm{sgn}(\Psi)\mathrm{e}^{\mathrm{i}\pi/4}}{8\pi^{1/2}(\delta^2+k_n^2)}\int_{-\infty}^{\infty}\left[4\mathrm{i}k_nC_4+4\mathrm{i}\delta C_3-\frac{(\lambda_1+w)^{1/2}f_2(\lambda_1)}{(\lambda_1-\lambda_2)(\lambda_1+\delta)^{1/2}(\lambda-\lambda_1)}\right.\\ \left.+\frac{(\lambda_2+\delta)f_2(\lambda_2)+\mathrm{i}k_nf_1(\lambda_2)}{(\lambda_1-\lambda_2)(\lambda_2-w)^{1/2}(\lambda_2+\delta')^{1/2}(\lambda-\lambda_2)}+\frac{(\lambda+w)^{1/2}f_2(\lambda)}{(\lambda+\delta)^{1/2}(\lambda-\lambda_1)(\lambda-\lambda_2)}\right]\frac{\mathrm{e}^{a(\lambda,\Phi,\Psi)}\mathrm{d}\lambda}{(\lambda+w)^{1/2}}.\end{aligned} \tag{A 10}$$

REFERENCES

ABRAMOWITZ, M. & STEGUN, I. A. 1972 *Handbook of Mathematical Functions*. Dover.

ASHLEY, H. & LANDAHL, M. 1985 *Aerodynamics of Wings and Bodies*. Dover.

ATASSI, H. M. 1984 The Sears problem for a lifting airfoil revisited – new results. *J. Fluid Mech.* **141**, 109–122.

ATASSI, H. M., SUBRAMANIAM, S. & SCOTT, J. R. 1990 Acoustic radiation from lifting airfoils in compressible subsonic flow. *AIAA Paper* 90-3911.

BATCHELOR, G. K. & PROUDMAN, I. 1954 The effect of rapid distortion of a fluid in turbulent motion. *Q. J. Mech. Appl. Maths* **1**, 83.

BLOKHINTSEV, D. I. 1946 Acoustics of a nonhomogeneous moving medium. English transl. *NACA Tech. Mem.* 1399.

CURLE, N. 1955 The influence of solid boundaries upon aerodynamic sound. *Proc. R. Soc. Lond.* A **231**, 505–514.

FFOWCS WILLIAMS, J. E. & HALL, L. H. 1970 Aerodynamic sound generation by turbulent flow in the vicinity of a scattering half-plane. *J. Fluid Mech.* **40**, 657–670.

FFOWCS WILLIAMS, J. E. & HAWKINGS, D. L. 1969*a* Sound generation by turbulence and surfaces in arbitrary motion. *Phil. Trans. R. Soc. Lond.* A **264**, 321–342.

FFOWCS WILLIAMS, J. E. & HAWKINGS, D. L. 1969*b* Theory relating to the noise of rotating machinery. *J. Sound Vib.* **10**, 10–21.

GOLDSTEIN, M. E. 1978 Unsteady vortical and entropic disturbances of potential flows round arbitrary obstacles. *J. Fluid Mech.* **89**, 433–468.

GOLDSTEIN, M. E. & ATASSI, H. 1976 A complete second order theory for the unsteady flow about an airfoil due to a periodic gust. *J. Fluid Mech.* **74**, 741–765.

GOLDSTEIN, M. E., ROSENBAUM, B. M. & ALBERS, L. U. 1974 Sound radiation from a high-speed axial-flow fan due to the inlet turbulence quadrupole interaction. *NASA TN* D-7667.

HUNT, J. C. R. 1973 A theory of turbulent flow round two-dimensional bluff bodies. *J. Fluid Mech.* **61**, 625–706.

KERSCHEN, E. J. & BALSA, T. F. 1981 Transformation of the equation governing disturbances of a two-dimensional compressible flow. *AIAA J.* **19**, 1367–1370.

KERSCHEN, E. J. & MYERS, M. R. 1987 Perfect gas effects in compressible rapid distortion theory. *AIAA J.* **25**, 504–507.

MORFEY, C. L. 1971 Acoustic energy in non-uniform flows. *J. Sound Vib.* **14**, 159–170.

MYERS, M. K. 1991 Transport of energy by disturbances in arbitrary steady flows. *J. Fluid Mech.* **226**, 383–400.

MYERS, M. R. & KERSCHEN, E. J. 1992 The acoustic field of a near-surface source at intermediate distances: a simple result using matched asymptotic expansions. *J. Acoust. Soc. Am.* **92**, 1743–1753.

MYERS, M. R. & KERSCHEN, E. J. 1995 Influence of camber on sound generation by airfoils interacting with high-frequency gusts. *J. Fluid Mech.* (to be submitted).

NOBLE, B. 1958 *Methods Based on the Wiener–Hopf Technique*. Pergamon.

SCOTT, J. R. & ATASSI, H. M. 1990 Numerical solution of the linearized Euler equations for unsteady vortical flows around lifting airfoils. *AIAA Paper* 90-0694.

VAN DER WAERDEN, B. L. 1951 On the method of saddle points. *Appl. Sci. Res.* **B2**, 33–45.

VAN DYKE, M. 1975 *Perturbation Methods in Fluid Mechanics*. Parabolic.